Journal of Medicinal Chemistry

Article

pubs.acs.org/jmc

# Synthesis and Evaluation of Novel $^{18}$F Labeled 2-Pyridinylbenzoxazole and 2-Pyridinylbenzothiazole Derivatives as Ligands for Positron Emission Tomography (PET) Imaging of $\beta$-Amyloid Plaques

Mengchao Cui,*[†,∥] Xuedan Wang,[†,∥] Pingrong Yu,[†] Jinming Zhang,[†,‡] Zijing Li,[†] Xiaojun Zhang,[‡] Yanping Yang,[†] Masahiro Ono,[§] Hongmei Jia,[†] Hideo Saji,[§] and Boli Liu*[†]

[†]Key Laboratory of Radiopharmaceuticals, Ministry of Education, College of Chemistry, Beijing Normal University, Beijing 100875, P. R. China

[‡]Department of Nuclear Medicine, Chinese PLA General Hospital, Beijing 100853, P. R. China

[§]Department of Patho-Functional Bioanalysis, Graduate School of Pharmaceutical Sciences, Kyoto University, 46-29 Yoshida Shimoadachi-cho, Sakyo-ku, Kyoto 606-8501, Japan

Supporting Information

**ABSTRACT:** A series of fluoro-pegylated (FPEG) 2-pyridinylbenzoxazole and 2-pyridinylbenzothiazole derivatives were synthesized and evaluated as novel $\beta$-amyloid (A$\beta$) imaging probes for PET. They displayed binding affinities for A$\beta_{1-42}$ aggregates that varied from 2.7 to 101.6 nM. Seven ligands with high affinity were selected for $^{18}$F labeling. In vitro autoradiography results confirmed the high affinity of these radiotracers. In vivo biodistribution experiments in normal mice indicated that the radiotracers with a short FPEG chain ($n$ = 1) displayed high initial uptake into and rapid washout from the brain. One of the 2-pyridinylbenzoxazole derivatives, [$^{18}$F]-5-(5-(2-fluoroethoxy)benzo[$d$]oxazol-2-yl)-$N$-methylpyridin-2-amine ([$^{18}$F]**32**) ($K_i$ = 8.0 ± 3.2 nM) displayed a brain$_{2min}$/brain$_{60min}$ ratio of 4.66, which is highly desirable for A$\beta$ imaging agents. Target specific binding of [$^{18}$F]**32** to A$\beta$ plaques was validated by ex vivo autoradiographic experiment with transgenic model mouse. Overall, [$^{18}$F]**32** is a promising A$\beta$ imaging agent for PET and merits further evaluation in human subjects.

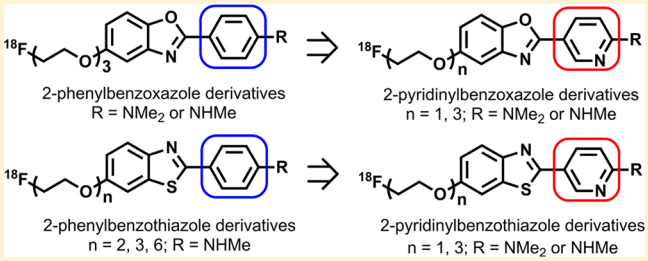


## INTRODUCTION

Alzheimer's disease (AD) is the most common form of dementia accounting for between 50% and over 70% of all cases among elderly people and is becoming an extensive health problem with the ever-increasing aging population. Clinically, AD is a lethal, progressive neurodegenerative disorder that leads to a decline in memory and many cognitive deficits, such as irreversible memory loss, impaired judgment, and problems with language. At present there are no treatments available to reverse or halt the progression of the disease. Although some drugs may provide temporary relief from symptoms, the benefit is limited. The best hope for progress might be to detect the disease at an early stage and initiate treatment before the brain damage is widespread. However, clinical diagnosis of AD is very difficult, and only possible or probable AD can be routinely diagnosed, while a definite diagnosis can only be made on biopsy and post-mortem brain tissue to confirm the existence of $\beta$-amyloid (A$\beta$) plaques and neurofibrillary tangles (NFTs). Although the etiology of AD has not been definitively established, the amyloid cascade hypothesis is the most prevailing theory to explain the pathogenesis of AD, which posits that the deposition of the A$\beta$ peptide in the brain is a crucial step that ultimately leads to AD.[1−5] Therefore, the development of novel imaging agents specifically targeting A$\beta$ plaques may lead to early diagnosis of AD and monitoring of the effectiveness of novel therapies for this devastating disease.[6−8]

In past decades, a number of radiolabeled A$\beta$ imaging agents based on highly conjugated A$\beta$ specific dyes, such as Congo Red (CR) and thioflavin T (Th-T), have been developed and reported for single photon emission computed tomography (SPECT) and positron emission tomography (PET),[9,10] some of which have been tested in humans (Figure 1). Among dozens of radioiodinated liagnds, [$^{123}$I]-6-iodo-2-(4′-dimethylamino)phenylimidazo[1,2]pyridine ([$^{123}$I]**1**, IMPY), a unique Th-T derivative with a [1,2,$a$]imidazopyridine ring, was the only SPECT tracer tested in humans. However, the signal-to-noise ratio for plaque labeling of [$^{123}$I]**1** in AD and healthy controls was not robust, while it was believed that the in vivo instability and fast metabolism of [$^{123}$I]**1** may ultimately lead to

Special Issue: Alzheimer's Disease

Received: July 6, 2012
Published: September 13, 2012

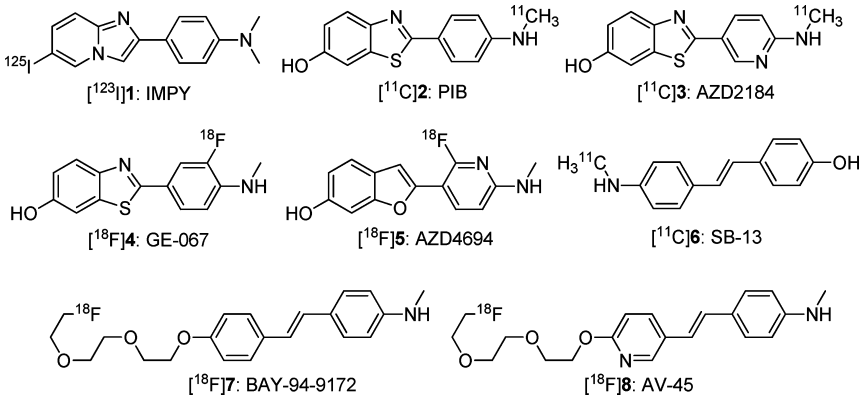


**Figure 1.** Structures of A$\beta$ imaging agents for SPECT and PET that have been evaluated in human subjects.

a decreasing of signal.[11−13] After that, there is no report of A$\beta$ imaging candidate for SPECT moving into clinical trial. In contrast, the development of radiotracers for PET imaging was more successful. [$^{11}$C]-2-(4-(Methylamino)phenyl)-6-hydroxybenzothiazol ([$^{11}$C]**2**, PIB), to date, is the most suitable and extensively studied PET radioligand for amyloid imaging and can distinguish AD from control cases clearly.[14−16] Recently, Andersson et al. reported a close analogue of [$^{11}$C]**2**, [$^{11}$C]-2-[6-(methylamino)pyridin-3-yl]-1,3-benzothiazol-6-ol ([$^{11}$C]**3**, AZD2184), by replacing the phenyl group with a pyridyl group, which displayed a decreased nonspecific binding in white matter.[17,18] Additionally, the stilbene scaffold, which could be considered as a more abbreviated form of CR, has also been selected for developing A$\beta$ imaging agents. Kung et. al reported the first $^{11}$C-labeled stilbene derivative, [$^{11}$C]-4-*N*-methylamino-4′-hydroxystilbene ([$^{11}$C]**6**, SB-13). Initial PET imaging in vivo with [$^{11}$C]**6** demonstrated potential usefulness in detecting A$\beta$ plaques in the human brain.[19,20] However, the short half-life of $^{11}$C ($T_{1/2}$ = 20 min) of the $^{11}$C-labeled tracers limits their usefulness for widespread clinical application. Thus, great efforts have been directed to developing imaging agents labeled with $^{18}$F ($T_{1/2}$ = 110 min). Two $^{18}$F-labeled PIB analogues, [$^{18}$F]-2-(3-fluoro-4-methyaminophenyl)-benzothiazol-6-ol ([$^{18}$F]**4**, GE-067)[21] and [$^{18}$F]-2-(2-fluoro-6-(methylamino)pyridin-3-yl)benzofuran-6-ol ([$^{18}$F]**5**, AZD4694),[22] are currently under phase II clinical testing in Europe. Meanwhile, two $^{18}$F-labeled stilbene derivatives with a short length of polyethylene glycol (PEG) units, [$^{18}$F]-4-(*N*-methylamino)-4′-(2-(2-(2-fluoroethoxy)ethoxy)ethoxy)stilbene ([$^{18}$F]**7**, BAY94-9172)[23] and [$^{18}$F]-(*E*)-4-(2-(6-(2-(2-(2-fluoroethoxy)ethoxy)ethoxy)pyridin-3-yl)vinyl)-*N*-methylaniline ([$^{18}$F]**8**, AV-45),[24−26] are under commercial development. More recently, [$^{18}$F]**8**, brand-named Amyvid by Eli Lilly, has been approved by the U.S. Food and Drug Administration (FDA).

Despite the fact that great success has been achieved on $^{18}$F-labeled tracers for amyloid imaging, it is clear that all $^{18}$F-labeled tracers show high levels of nonspecific white matter retention than [$^{11}$C]**2**. In AD patients, the average cortical binding is similar to or less than the uptake in white matter and may limit the sensitivity of PET imaging.[27] The mechanism of white matter retention seems to be owing to nonspecific binding that to some degree is governed by the lipophilicity of the ligand.[22] Thus, further modifications in order to decrease lipophilicity are needed. Two approaches were used to decrease the lipophilicity of $^{18}$F-labeled ligand: (1) introducing a short length of PEG ($n$ = 2−12) and capping the end of the ethylene glycol chain with a fluorine atom [fluoropolyethylene glycol (FPEG)], which will provide a flexible tool to adjust lipophilicity and to maintain a relatively small size;[28] (2) displacing one of the benzene rings of ligand with one pyridine ring. Previous work indicates that the in vivo pharmacokinetics of the fluoro-pegylated pyridylbenzofuran derivatives ([$^{18}$F]**11**, [$^{18}$F]**12**)[29,30] were greatly improved compared with the phenylbenzofuran derivatives ([$^{18}$F]**9**, [$^{18}$F]**10**).[31] Tracer [$^{18}$F]**12** displayed the best pharmacokinetics of radioactivity in the brain, with the brain$_{2min}$/brain$_{60min}$ ratio being 2.34. Kung et. al also reported a series of fluoro-pegylated phenylbenzothiazole derivatives ([$^{18}$F]**15**−**17**) with improved properties compared with the original radioiodinated ligand[28] (Figure 2).

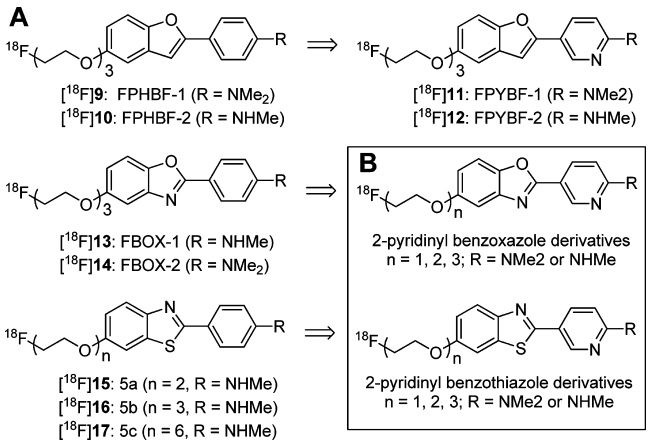


**Figure 2.** (A) Structures of radiolabeled benzofuran, benzoxazole, and benzothiazole derivatives. (B) Structures of the designed $^{18}$F-labeled 2-pyridinylbenzoxazole and 2-pyridinylbenzothiazole derivatives.

In an attempt to further explore more promising $^{18}$F-labeled tracers, we extended our fluoro-pegylation approach from benzofuran to benzoxazole. The strategy of FPEG was successfully applied to the benzoxazole scaffold, and it has been demonstrated that the fluoro-pegylated phenylbenzoxazole derivatives ([$^{18}$F]**13**, [$^{18}$F]**14**) showed more promising in vivo kinetics than the corresponding radioiodinated ligand and the benzofuran derivatives.[32] Tracer [$^{18}$F]**13** with a monomethylamino group exhibited high affinity for A$\beta$ aggregates ($K_i$ = 9.3 nM) and high initial uptake into the brain and displayed excellent binding to A$\beta$ plaques in ex vivo autoradiographic experiments with Tg2576 mice. What's more, small-animal


dx.doi.org/10.1021/jm300973k | J. Med. Chem. 2012, 55, 9283−9296

**Scheme 1**[a]

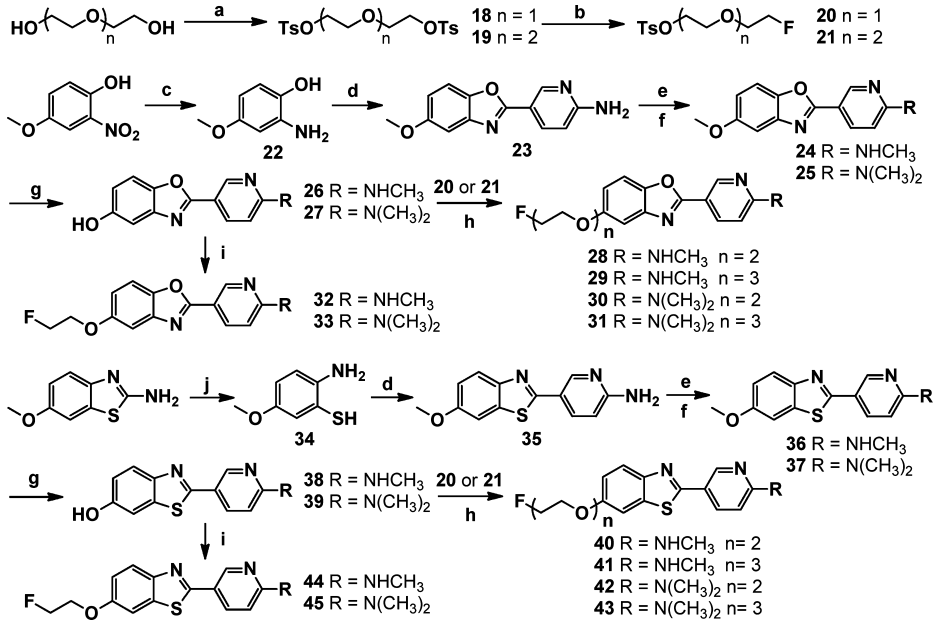


[a]Reagents and conditions: (a) TsCl, KOH, $CH_2Cl_2$, 0 °C to rt; (b) TBAF (1 M in THF), THF, reflux; (c) Pd/C, MeOH, rt; (d) 2-amino-5-(trifluoromethyl)pyridine, NaOH (1 M), $H_2O$, reflux; (e) (1) NaOMe, MeOH, $(CH_2O)_n$, reflux; (2) $NaBH_4$, rt; (f) $NaBH_3CN$, $(CH_2O)_n$, $CH_3COOH$, rt; (g) $BBr_3$ (1 M in $CH_2Cl_2$), $CH_2Cl_2$, −78 °C to rt; (h) $K_2CO_3$, DMF, 110 °C; (i) 1-bromo-2-fluoroethane, $K_2CO_3$, DMF, 110 °C; (j) KOH, $H_2O$, reflux.

**Scheme 2**[a]

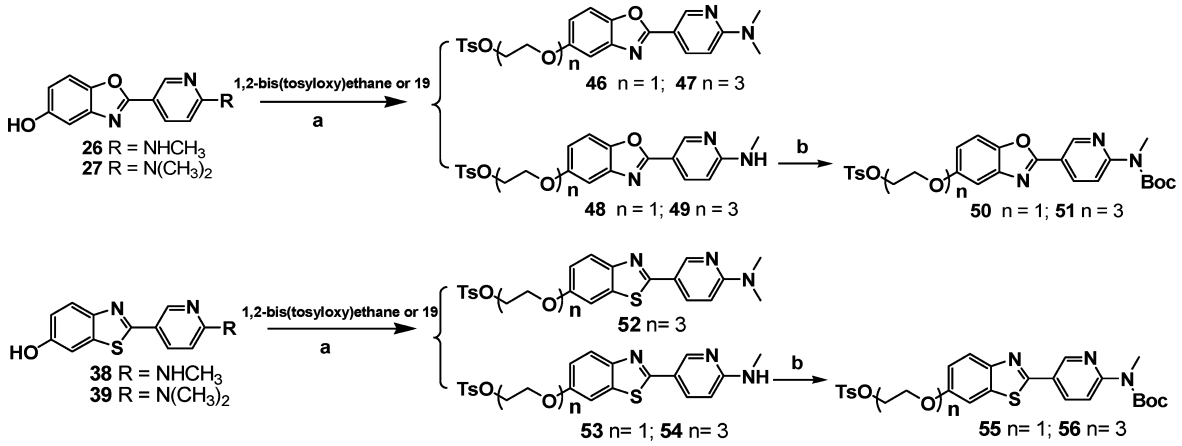


[a]Reagents and conditions: (a) $K_2CO_3$, 18-crown-6, acetone, reflux; (b) $(Boc)_2O$, THF, reflux.

PET studies demonstrated significant differences between Tg2576 and wild-type mice in the clearance profiles after the administration of [$^{18}$F]**13**. Although the preliminary results indicate that [$^{18}$F]**13** is a promising PET tracer for imaging A$\beta$ plaques, the $brain_{2min}/brain_{60min}$ ratio of [$^{18}$F]**13** (2.67) was still lower than that of [$^{18}$F]**8** (3.90). To further improve the pharmacokinetic profile of the fluoro-pegylated phenylbenzothiazole and phenylbenzoxazole derivatives, we decided to use the strategy of bioisosteric replacement by displacing the phenyl group with a pyridyl group to reduce nonspecific binding in white matter and enhance the signal-to-noise ratio. We report herein the synthesis and the initial biological evaluation of fluoro-pegylated pyridylbenzothiazole and pyridylbenzoxazole derivatives as novel PET imaging probes targeting A$\beta$ plaques in the brain.

## RESULTS AND DISCUSSION

**Chemistry.** The synthesis of fluoro-pegylated pyridylbenzothiazole and pyridylbenzoxazole derivatives is outlined in Scheme 1. The intermediates **20** and **21** were obtained by ready fluorination of the oligoethylene glycol ditosylate ester (**18**, **19**) using anhydrous tetra-*n*-butylammonium fluoride in THF. The desired 2-aminopyridylbenzothiazole and 2-aminopyridylbenzoxazole core structures (**23** and **35**) were obtained by using a previously reported one-step reaction between 5-(trifluoromethyl)pyridin-2-amine and 2-amino-4-methoxyphenol (**22**) or 2-amino-5-methoxybenzenethiol (**34**) in aqueous NaOH solution with excellent yields (89 and 50%, respectively).[33] Conversion of **23** and **35** to the monomethylamino derivatives **24** and **36** was achieved by the monomethylation of the amino group by using a method


dx.doi.org/10.1021/jm300973k | J. Med. Chem. 2012, 55, 9283−9296

Scheme 3[a]

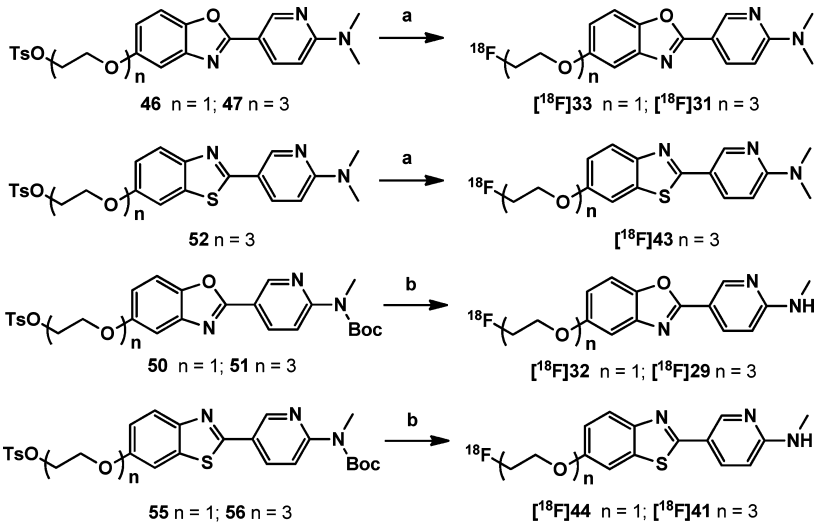


[a]Reagents and conditions: (a) $^{18}F^-$, $K_2CO_3$, Kryptofix 222, acetonitrile, 100 °C; (b) (1) $^{18}F^-$, $K_2CO_3$, Kryptofix 222, acetonitrile, 100 °C; (2) HCl (1 M), 100 °C.

previously reported in yields of 98% and 98%, respectively.[34] The dimethylamino derivatives **25** and **37** were prepared by an efficient dimethylation method with paraformaldehyde, sodium cyanoborohydride, and acetic acid (89% and 91%, respectively). The *O*-methyl groups of **24**, **25**, **36**, and **37** were removed by reacting with $BBr_3$ in $CH_2Cl_2$ to give **26**, **27**, **38**, and **39** in yields of 97%, 89%, 88%, and 68%, respectively. Then the hydroxy groups were coupled with 1-bromo-2-fluoroethane to give the fluorinated derivatives (**32**, **33**, **44**, and **45**) with one ethoxy unit as the PEG linkage. The corresponding fluorinated derivatives with two or three ethoxy units (**28**–**31** and **40**–**43**) were prepared by the hydroxyl compounds with $K_2CO_3$ and the intermediate **20** or **21** in DMF (yield, 40–75%).

The synthesis of tosylate precursors is outlined in Scheme 2. The free hydroxy groups present in **26**, **27**, **38**, and **39** were coupled with ethane-1,2-diyl bis(4-methylbenzenesulfonate) or **19** in acetone catalyzed by 18-crown-6 to give **46**–**49** and **52**–**54** (yield, 28–49%). For the monomethylated precursors, the methylamino groups of intermediates **48**, **49**, **53**, and **54** were protected by a butyloxycarbonyl (BOC) group to give the tosylate precursors **50**, **51**, **55**, and **56** in yields of 67%, 23%, 80%, and 63%, respectively. Compared with the synthesis routes for the precursors of benzofuran and benzoxazole derivatives, the procedures reported here are much simpler, while some protection and deprotection steps were not needed.

**Radiolabeling.** To make the desired $^{18}F$-labeled dimethylamino tracers [$^{18}F$]**33**, [$^{18}F$]**31**, and [$^{18}F$]**43**, tosylate precursors **46**, **47**, and **52** were reacted with [$^{18}F$]fluoride/potassium carbonate and Kryptofix 222 in acetonitrile with radiochemical yields of 53%, 57%, and 46%, respectively. For the monomethylamino tracers [$^{18}F$]**32**, [$^{18}F$]**29**, [$^{18}F$]**44**, and [$^{18}F$]**41**, the *N*-Boc-protected tosylates **50**, **51**, **55**, and **56** were employed as the precursors. After [$^{18}F$]fluorination, the mixture was treated with aqueous HCl to remove the *N*-BOC-protecting group (radiochemical yields, 41%, 21%, 33%, and 27%, respectively). The radiochemical purity of these radiotracers was greater than 98% after purification by high performance liquid chromatography (HPLC), and their specific activity was estimated as approximately 200 GBq/$\mu$mol. The identity of $^{18}F$-labeled tracers was verified by a comparison of the retention time with that of the nonradioactive compound (see Supporting Information) (Scheme 3).

**In Vitro Binding Studies.** The affinities of these fluoropegylated pyridylbenzothiazole and pyridylbenzoxazole derivatives (**28**–**33** and **40**–**45**) for A$\beta_{1-42}$ aggregates were examined with competition binding assays using [$^{125}$I]**1** as the competing radioligand. IMPY and PIB were also screened using the same system for comparison. As shown in Table 1, all ligands with a dimethylamino group (**30**, **31**, **33**, **42**, **43**, and **45**) displayed high binding affinity to A$\beta_{1-42}$ aggregates ($K_i$ < 10.0 nM). Similar to the findings reported previously,[30] the tertiary *N*,*N*-dimethylamino analogues were found to have higher affinities than their secondary *N*-methylamino analogues, especially for the pyridylbenzoxazole derivatives (e.g., **28** vs **30**, **29** vs **31**, **32** vs **33**). The length of the FPEG chain did not bring about an appreciable progress in the binding affinity to amyloid

**Table 1. Inhibition Constants of Fluorinated 2-Pyridinylbenzoxazole and 2-Pyridinylbenzothiazole Derivatives for the Binding of [$^{125}$I]IMPY to A$\beta_{1-42}$ Aggregates**

| compd | $K_i$ ± SEM (nM)[a] |
|---|---|
| **28** | 101.6 ± 15.3 |
| **29** | 76.9 ± 15.5 |
| **30** | 7.3 ± 0.8 |
| **31** | 9.9 ± 0.5 |
| **32** | 8.0 ± 3.2 |
| **33** | 2.7 ± 0.7 |
| **40** | 29.7 ± 7.1 |
| **41** | 9.3 ± 0.1 |
| **42** | 4.6 ± 0.6 |
| **43** | 5.8 ± 1.8 |
| **44** | 10.1 ± 2.4 |
| **45** | 2.7 ± 0.6 |
| IMPY | 10.5 ± 1.0[b] |
| PIB | 9.0 ± 1.3[b] |

[a]The $K_i$ values were determined in three independent experiments ($n$ = 3) unless otherwise noted. [b]Data from ref 30.


dx.doi.org/10.1021/jm300973k | J. Med. Chem. 2012, 55, 9283–9296

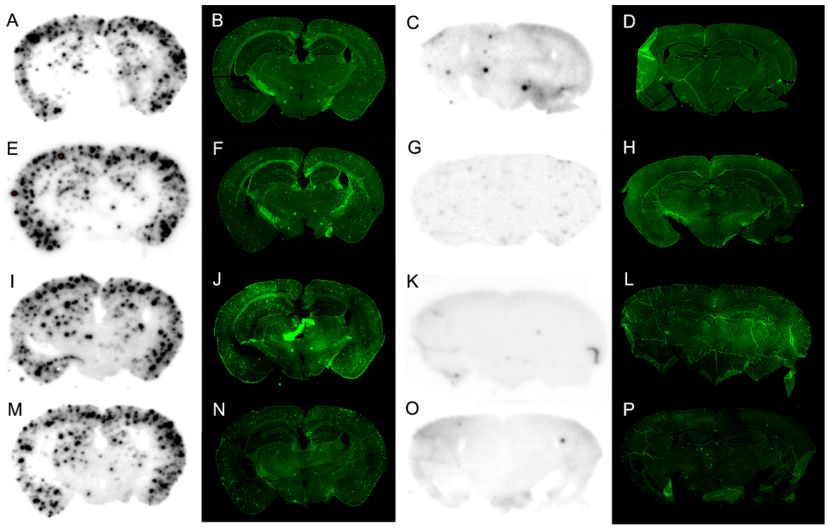


**Figure 3.** In vitro autoradiography of $^{18}$F-labeled 2-pyridinylbenzoxazole derivatives ([$^{18}$F]**29**, [$^{18}$F]**31**, [$^{18}$F]**32**, and [$^{18}$F]**33**) on a Tg model mouse (C57BL6, APPswe/PSEN1, 12 months old, male) (A, E, I, M) and normal control mouse (C57BL6, 12 months old, male) (C, G, K, O). The presence and distribution of plaques in the sections were confirmed by fluorescence staining using thioflavin S on the same sections with a filter set for GFP (B, D, F, H, J, L, N, P).

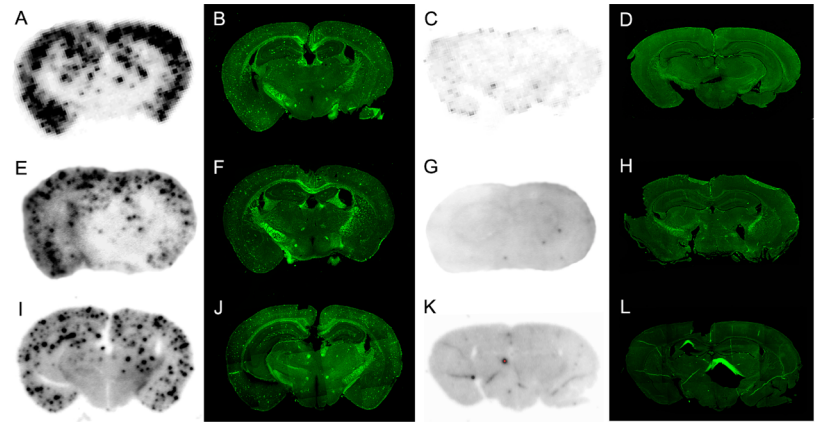


**Figure 4.** In vitro autoradiography of $^{18}$F-labeled 2-pyridinylbenzothiazole derivatives ([$^{18}$F]**41**, [$^{18}$F]**43**, and [$^{18}$F]**44**) on a Tg model mouse (C57BL6, APPswe/PSEN1, 12 months old, male) (A, E, I) and normal control mouse (C57BL6, 12 months old, male) (C, G, K). The presence and distribution of plaques in the sections were confirmed by fluorescence staining using thioflavin S on the same sections with a filter set for GFP (B, D, F, H, J, L).

aggregates for the pyridylbenzothiazole derivatives (**40**–**45**). However, the length of the FPEG chain is very important for the secondary *N*-methylamino analogues of pyridylbenzoxazole. The binding affinities were reduced dramatically with the addition of the FPEG chain [e.g., **28** ($K_i$ = 101.6 ± 15.3 nM) and **29** ($K_i$ = 76.9 ± 15.5 nM)], while **32** retained high binding affinity for the $n$ = 1 FPEG conjugates ($K_i$ = 8.0 ± 3.2 nM). On the basis of the high binding affinity to A$\beta_{1-42}$ aggregates, ligands **29**, **31**, **32**, **33**, **41**, **43**, and **44** were selected for $^{18}$F labeling.

**In Vitro Autoradiography Studies.** In vitro autoradiographic studies of the $^{18}$F-labeled tracers were first performed with sections of Tg mice (C57BL6, APPswe/PSEN1, 12 months old) and an age-matched control mice. As shown in Figures 3 and 4, all of the $^{18}$F-labeled tracers displayed excellent labeling of A$\beta$ plaques in the hippocampus and cortical regions of the Tg mice and lack of any notable A$\beta$ labeling in control mice. The distribution of A$\beta$ plaques was consistent with the results of fluorescent staining with thioflavin S. A previous report suggested that the configuration/folding of A$\beta$ plaques in Tg mice might be different from the tertiary/quaternary structure of A$\beta$ plaques in AD brains.[35] Thus, the binding information for A$\beta$ plaques in human AD brain is important. Tracers [$^{18}$F]**29**, [$^{18}$F]**32**, [$^{18}$F]**41**, and [$^{18}$F]**44** with a monomethylamino group were selected for autoradiographic studies in sections of human brain tissue. As shown in Figure 5, a highly dense labeling of plaques was observed in AD brain sections. In contrast, no apparent labeling was observed in normal adult brain sections. Although the binding affinity of [$^{18}$F]**29** to A$\beta$ aggregates was not potent ($K_i$ = 76.9 ± 15.5 nM), [$^{18}$F]**29** was still able to label the plaques in sections of Tg mice and AD.

**In Vivo Biodistribution Studies.** Biodistribution study of the radiolabeled tracers in normal mice is often used as a test to measure the initial brain uptake [ability to penetrate intact blood–brain barrier (BBB)] and washout kinetics from the normal brain. The time–activity data on the brain permeation as well as the other organ distribution of the $^{18}$F-labeled tracers acquired in normal ICR mice after intravenous administration are summarized in Tables 2–4. [$^{18}$F]**32**, [$^{18}$F]**33**, and [$^{18}$F]**44**


dx.doi.org/10.1021/jm300973k | J. Med. Chem. 2012, 55, 9283–9296

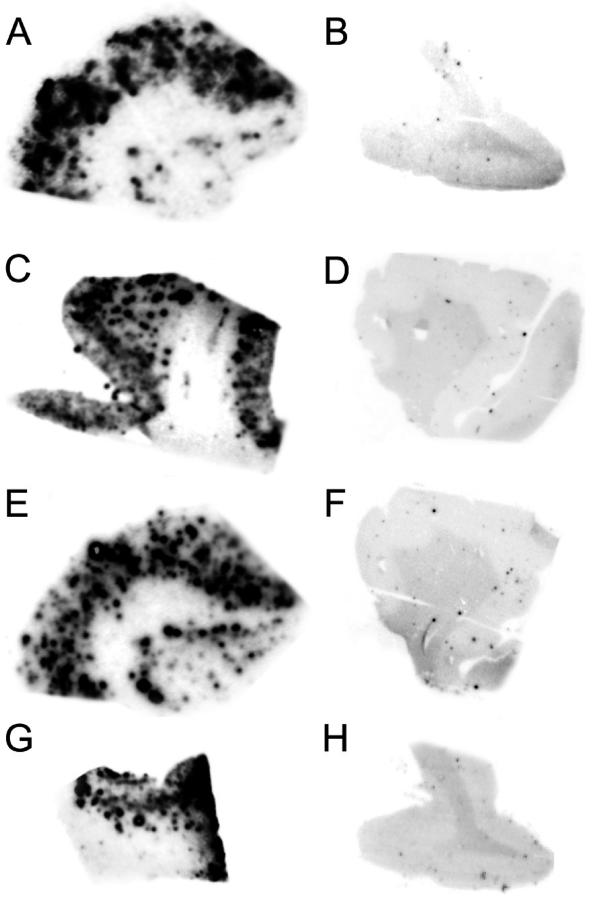


**Figure 5.** In vitro autoradiography of [$^{18}$F]**29** (A), [$^{18}$F]**32** (C), [$^{18}$F]**41** (E), and [$^{18}$F]**44** (G) on human brain sections: (A, C, E, G) postmortem AD cases; (B, D, F, H) normal control.

with a short FPEG chain ($n$ = 1) displayed high uptakes into the brain (7.23, 7.27, and 7.87% ID/g, respectively) at 2 min postinjection and fast washout kinetics from the healthy brain (1.55, 1.47, and 2.83% ID/g at 60 min, respectively). These values were comparable to those reported for the $^{18}$F-labeled pyridylbenzofuran ([$^{18}$F]**10**, [$^{18}$F]**12**)[30] and phenylbenzoxazole ([$^{18}$F]**13**)[32] derivatives as well as [$^{18}$F]**7** and [$^{18}$F]**8**, which are under commercial development. The ratio $\text{brain}_{2\text{min}}/\text{brain}_{60\text{min}}$ is considered as an important index with which to select tracers with appropriate kinetics in vivo. These three tracers showed $\text{brain}_{2\text{min}}/\text{brain}_{60\text{min}}$ ratios of 4.66, 4.95, and 2.78, respectively, indicating that the pyridylbenzoxazole scaffold is more potent than pyridylbenzothiazole. However, the BBB penetration ability of the $^{18}$F-labeled tracers with a long FPEG chain ($n$ = 3) ([$^{18}$F]**29**, [$^{18}$F]**31**, [$^{18}$F]**41**, and [$^{18}$F]**43**) was decreased (4.05, 3.79, 2.23, and 3.26% ID/g at 2 min, respectively). The FPEG strategy was used to modulate the lipophilicity of $^{18}$F-labeled tracers. As reflected in log $D$ values, the lipophilicity of the tracers with a long FPEG chain decreased slightly, which may explain the lower brain uptake. Moreover, the flexiblility and polar properties of the long FPEG chain may also interfere and limit brain penetration.[28] It was also observed that in vivo defluorination was likely occurring with [$^{18}$F]**31** and [$^{18}$F]**44** because the bone uptakes increased with time (6.39 and 6.70% dose/g at 1 h, respectively). However, they were minimal compared to other $^{18}$F-labeled tracers, so the interference with the imaging is expected to be relatively minor. These $^{18}$F-labeled tracers were also distributed to several other organs. The high initial uptakes in the liver and the kidneys were followed by a moderate washout, while the uptake in the intestines showed an accumulation of radioactivity over time. In summary, two of the $^{18}$F-labeled pyridylbenzoxazole derivatives ([$^{18}$F]**32** and [$^{18}$F]**33**) meet the preliminary requirements for a potential PET imaging agent for in vivo detection of A$\beta$ plaque. Compared with the $^{18}$F-labeled pyridylbenzofuran, phenylbenzoxazole, and phenylbenzothiazol derivatives, the $^{18}$F-labeled pyridylbenzoxazole derivatives had greatly improved pharmacokinetics. In addition, the $\text{brain}_{2\text{min}}/\text{brain}_{60\text{min}}$ ratio of [$^{18}$F]**32** and [$^{18}$F]**33** was superior than that of [$^{18}$F]**8** (3.90).

**Ex Vivo Autoradiography Studies.** A previous report suggested that a rapid metabolism in vivo of the dimethylamino group in the tracer may occur,[36] and most of the radiotracers for A$\beta$ plaques in clinical trials have a monomethylamino group. For the same reason, [$^{18}$F]**32** was selected for further ex vivo autoradiography studies in Tg mice (C57BL6, APPswe/PSEN1, 10 months old) and wild-type mice (C57BL6, 10 months old). As shown in Figure 6A and Figure 6C, the A$\beta$ plaques in the cortical regions of Tg mice were clearly labeled by [$^{18}$F]**32**, while wild-type mouse brain showed no such labeling (Figure 6E). The labeling of the plaques was confirmed by costaining with thioflavin S on the same sections (Figure 6B and Figure 6D).

**In Vitro Stability Studies.** In vitro stability study of [$^{18}$F]**32** in saline solution indicated that [$^{18}$F]**32** solutions were stable during storage for at least 6 h at room temperature. Moreover, [$^{18}$F]**32** was found to have high in vitro stability in mice plasma; more than 95% of the activity was identified as the intact tracer after 60 min of incubating with mice plasma at 37 °C (see Supporting Information).

## CONCLUSIONS

A series of fluoro-pegylated (FPEG) 2-pyridinylbenzoxazole and 2-pyridinylbenzothiazole derivatives had been successfully prepared and evaluated as PET imaging tracers for A$\beta$ plaques. In binding studies, they displayed binding affinities for A$\beta$ aggregates that varied from 2.7 to 101.6 nM. Seven ligands with high affinity (**29**, **31**, **32**, **33**, **41**, **43**, and **44**) were selected for $^{18}$F labeling. In vitro autoradiography with sections of postmortem AD brain and Tg mouse brain confirmed the affinity of these tracers. In biodistribution experiments using normal mice, the radiotracers with a short FPEG chain ($n$ = 1) displayed high initial uptake into and rapid washout from the brain in normal mice. However, the BBB penetration ability of the $^{18}$F-labeled tracers with a long FPEG chain ($n$ = 3) was not robust. Compared with the $^{18}$F-labeled pyridylbenzofuran, phenylbenzoxazole, and phenylbenzothiazol derivatives, the $^{18}$F-labeled pyridylbenzoxazole derivatives had greatly improved pharmacokinetics. On the basis of the above results, one of the 2-pyridinylbenzoxazole derivatives, [$^{18}$F]**32** ($K_i$ = 8.0 ± 3.2 nM), displayed a $\text{brain}_{2\text{min}}/\text{brain}_{60\text{min}}$ ratio of 4.66, which is highly desirable for A$\beta$ imaging agents. Target specific binding of [$^{18}$F]**32** to A$\beta$ plaques was validated by ex vivo autoradiographic experiments with Tg mouse. Furthermore, [$^{18}$F]**32** displayed high in vitro stability in saline solution and mice plasma. Overall, [$^{18}$F]**32** is a promising PET imaging agent for cerebral A$\beta$ plaques and merits further evaluation in human subjects.

## EXPERIMENTAL SECTION

**General Remarks.** All reagents used in the synthesis were commercial products and were used without further purification

Table 2. Biodistribution in Normal ICR Mice after Intravenous Injection of the $^{18}$F-Labeled 2-Pyridinylbenzoxazole Tracers[a]

| organ | 2 min | 10 min | 30 min | 60 min |
|---|---|---|---|---|
| | | [$^{18}$F]**29** (log $D$ = 2.86 ± 0.12) | | |
| blood | 5.07 ± 0.41 | 3.04 ± 0.29 | 3.16 ± 0.26 | 2.74 ± 0.24 |
| brain | 4.05 ± 0.36 | 2.05 ± 0.27 | 2.06 ± 0.29 | 1.78 ± 0.21 |
| heart | 5.50 ± 0.70 | 3.35 ± 0.37 | 3.16 ± 0.28 | 2.50 ± 0.27 |
| liver | 14.22 ± 2.65 | 9.32 ± 0.79 | 6.47 ± 0.72 | 4.21 ± 0.66 |
| spleen | 4.13 ± 0.32 | 2.64 ± 0.35 | 2.18 ± 0.11 | 1.79 ± 0.16 |
| lung | 5.30 ± 0.31 | 3.15 ± 0.46 | 2.81 ± 0.24 | 2.34 ± 0.19 |
| kidney | 8.51 ± 0.97 | 4.79 ± 0.57 | 3.73 ± 0.20 | 2.54 ± 0.33 |
| stomach[b] | 5.08 ± 0.98 | 12.32 ± 0.85 | 12.93 ± 1.25 | 12.02 ± 1.82 |
| intestine[b] | 10.81 ± 0.86 | 22.90 ± 1.90 | 28.65 ± 2.66 | 25.16 ± 0.97 |
| bone | 1.75 ± 0.25 | 1.92 ± 0.65 | 2.46 ± 0.33 | 3.93 ± 0.48 |
| | | [$^{18}$F]**31** (log $D$ = 3.26 ± 0.04) | | |
| blood | 5.47 ± 0.56 | 3.05 ± 0.25 | 2.74 ± 0.14 | 2.87 ± 0.12 |
| brain | 3.79 ± 0.41 | 1.97 ± 0.14 | 1.85 ± 0.06 | 1.82 ± 0.07 |
| heart | 5.24 ± 0.63 | 3.51 ± 0.11 | 2.97 ± 0.18 | 2.73 ± 0.13 |
| liver | 13.25 ± 3.13 | 5.41 ± 0.67 | 7.24 ± 2.05 | 3.46 ± 1.52 |
| spleen | 3.00 ± 0.63 | 2.69 ± 0.65 | 2.41 ± 0.10 | 2.34 ± 0.26 |
| lung | 3.03 ± 0.63 | 2.34 ± 0.66 | 2.64 ± 0.29 | 1.87 ± 0.66 |
| kidney | 8.27 ± 2.03 | 5.14 ± 0.30 | 4.20 ± 0.42 | 3.21 ± 0.46 |
| stomach[b] | 2.66 ± 0.60 | 5.10 ± 0.80 | 9.26 ± 2.63 | 6.45 ± 1.79 |
| intestine[b] | 8.13 ± 0.79 | 14.45 ± 2.65 | 28.15 ± 3.11 | 28.54 ± 4.18 |
| bone | 1.79 ± 0.36 | 2.70 ± 0.47 | 4.71 ± 0.34 | 6.39 ± 0.57 |
| | | [$^{18}$F]**32** (log $D$ = 3.52 ± 0.13) | | |
| blood | 3.36 ± 0.15 | 2.55 ± 0.15 | 2.55 ± 0.17 | 3.20 ± 0.48 |
| brain | 7.23 ± 0.04 | 2.24 ± 0.12 | 1.69 ± 0.17 | 1.55 ± 0.17 |
| heart | 4.66 ± 0.34 | 2.34 ± 0.17 | 1.84 ± 0.19 | 2.05 ± 0.21 |
| liver | 10.48 ± 1.65 | 8.50 ± 0.72 | 3.95 ± 0.66 | 2.64 ± 0.86 |
| spleen | 3.32 ± 0.50 | 2.13 ± 0.24 | 1.63 ± 0.28 | 1.64 ± 0.13 |
| lung | 4.14 ± 0.24 | 2.80 ± 0.48 | 2.29 ± 0.09 | 2.57 ± 0.40 |
| kidney | 7.45 ± 0.35 | 3.52 ± 0.52 | 2.17 ± 0.22 | 3.04 ± 0.99 |
| stomach[b] | 3.24 ± 0.62 | 5.59 ± 1.45 | 3.11 ± 0.94 | 3.89 ± 1.58 |
| intestine[b] | 9.87 ± 0.97 | 19.61 ± 2.42 | 33.66 ± 5.26 | 39.05 ± 6.70 |
| bone | 1.18 ± 0.21 | 1.11 ± 0.36 | 2.34 ± 0.88 | 2.37 ± 0.86 |
| | | [$^{18}$F]**33** (log $D$ = 3.53 ± 0.04) | | |
| blood | 3.57 ± 0.39 | 2.05 ± 0.10 | 1.89 ± 0.17 | 2.06 ± 0.26 |
| brain | 7.27 ± 0.19 | 3.41 ± 0.36 | 1.76 ± 0.16 | 1.47 ± 0.25 |
| heart | 5.95 ± 0.95 | 2.44 ± 0.18 | 1.83 ± 0.24 | 1.93 ± 0.21 |
| liver | 15.70 ± 2.71 | 10.72 ± 1.44 | 4.39 ± 0.80 | 3.19 ± 0.61 |
| spleen | 3.22 ± 0.52 | 2.02 ± 0.25 | 1.60 ± 0.14 | 1.32 ± 0.26 |
| lung | 5.53 ± 0.50 | 2.58 ± 0.31 | 1.85 ± 0.46 | 1.79 ± 0.38 |
| kidney | 8.48 ± 0.77 | 3.82 ± 0.37 | 2.44 ± 0.59 | 1.82 ± 0.34 |
| stomach[b] | 2.44 ± 0.76 | 2.55 ± 0.82 | 2.54 ± 0.48 | 2.79 ± 0.57 |
| intestine[b] | 8.41 ± 1.83 | 21.45 ± 6.22 | 38.88 ± 2.94 | 37.02 ± 6.37 |
| bone | 2.08 ± 0.73 | 1.27 ± 0.15 | 1.56 ± 0.53 | 1.88 ± 0.39 |

[a]Expressed as % injected dose per gram unless otherwise indicated. Data are the average for five mice ± standard deviation. [b]Expressed as % injected dose per organ.

unless otherwise indicated. The $^1$H NMR spectra were obtained at 400 MHz on Bruker spectrometer in $CDCl_3$ or DMSO-$d_6$ solutions at room temperature with TMS as an internal standard. Chemical shifts were reported as $\delta$ values relative to the internal TMS. Coupling constants were reported in hertz. Multiplicity is defined by s (singlet), d (doublet), t (triplet), and m (multiplet). Mass spectra were acquired under a SurveyorMSQ Plus (ESI) instrument. Radiochemical purity was determined by HPLC performed on a Shimadzu system SCL-20 AVP equipped with a SPD-20A UV detector ($\lambda$ = 254 nm) and Bioscan flow count 3200 NaI/PMT $\gamma$-radiation scintillation detector. HPLC separations were achieved on a Venusil MP C18 reverse phase column (Agela Technologies, 5 $\mu$m, 10 mm × 250 mm), and elution was with a binary gradient system at a flow rate of 4.0 mL/min. HPLC analyses were achieved on a Venusil MP C18 reverse phase column (Agela Technologies, 5 $\mu$m, 4.6 mm × 250 mm), and elution was with a binary gradient system at a flow rate of 1.0 mL/min. Mobile phase A was water, while mobile phase B was acetonitrile. The purity of the synthesized key compounds (**28**−**33** and **40**−**45**) was determined using analytical HPLC and was found to be more than 96%. Fluorescent observation was performed by the Oberver Z1 (Zeiss, Germany) equipped with GFP filter set (excitation, 505 nm). Normal ICR mice (5 weeks, male) were used for biodistribution experiments. Transgenic mice (C57BL6, APPswe/PSEN1, 12 months old), used as an Alzheimer's model, were purchased from the Institute of Laboratory Animal Science, Chinese Academy of Medical Sciences. All protocols requiring the use of mice were approved by the Animal Care Committee of Beijing Normal University.

**Chemistry. 2,2′-Oxybis(ethane-2,1-diyl) Bis(4-methylbenzenesulfonate) (18).** Intermediate **18** was synthesized according to the literature.[37] Briefly, to a solution of tosyl chloride (19.8 g, 10 mmol)


dx.doi.org/10.1021/jm300973k | J. Med. Chem. 2012, 55, 9283−9296

Table 3. Biodistribution in Normal ICR Mice after Intravenous Injection of the $^{18}$F-Labeled 2-Pyridinylbenzothiazole Tracers[a]

| organ | 2 min | 10 min | 30 min | 60 min |
|---|---|---|---|---|
| | | [$^{18}$F]**41** (log $D$ = 2.85 ± 0.07) | | |
| blood | 6.92 ± 0.60 | 4.25 ± 0.32 | 3.49 ± 0.11 | 2.94 ± 0.19 |
| brain | 2.23 ± 0.33 | 1.63 ± 0.15 | 1.31 ± 0.17 | 1.26 ± 0.15 |
| heart | 3.53 ± 0.36 | 2.16 ± 0.16 | 1.96 ± 0.13 | 1.85 ± 0.13 |
| liver | 15.22 ± 2.34 | 9.38 ± 0.90 | 8.16 ± 0.46 | 4.12 ± 0.65 |
| spleen | 2.68 ± 0.35 | 2.05 ± 0.24 | 1.74 ± 0.07 | 1.49 ± 0.15 |
| lung | 5.53 ± 0.26 | 3.36 ± 0.50 | 3.11 ± 0.06 | 1.93 ± 0.43 |
| kidney | 6.02 ± 0.98 | 4.04 ± 0.39 | 3.12 ± 0.25 | 2.66 ± 0.23 |
| stomach[b] | 2.96 ± 0.62 | 9.44 ± 1.92 | 11.46 ± 3.60 | 8.78 ± 1.46 |
| intestine[b] | 5.69 ± 0.98 | 10.06 ± 0.62 | 21.68 ± 2.74 | 18.60 ± 4.73 |
| bone | 1.19 ± 0.42 | 0.86 ± 0.11 | 1.33 ± 0.32 | 1.42 ± 0.17 |
| | | [$^{18}$F]**43** (log $D$ = 3.08 ± 0.01) | | |
| blood | 9.79 ± 0.81 | 5.44 ± 0.16 | 4.96 ± 0.87 | 3.79 ± 0.37 |
| brain | 3.26 ± 0.21 | 2.64 ± 0.19 | 1.98 ± 0.20 | 1.84 ± 0.22 |
| heart | 4.50 ± 0.67 | 3.30 ± 0.17 | 2.62 ± 0.11 | 2.02 ± 0.98 |
| liver | 12.90 ± 0.62 | 11.60 ± 0.71 | 6.79 ± 0.80 | 4.75 ± 0.39 |
| spleen | 3.14 ± 0.32 | 2.97 ± 0.23 | 2.59 ± 0.55 | 1.47 ± 0.77 |
| lung | 6.69 ± 0.53 | 4.59 ± 0.34 | 3.28 ± 0.95 | 2.33 ± 0.94 |
| kidney | 6.82 ± 0.61 | 5.45 ± 0.32 | 3.88 ± 0.89 | 3.01 ± 0.61 |
| stomach[b] | 2.55 ± 0.54 | 8.98 ± 0.14 | 14.13 ± 0.61 | 11.34 ± 0.98 |
| intestine[b] | 4.68 ± 0.23 | 10.4 ± 1.27 | 19.57 ± 1.68 | 26.66 ± 2.90 |
| bone | 1.86 ± 0.27 | 0.95 ± 0.48 | 1.64 ± 0.28 | 1.58 ± 0.28 |
| | | [$^{18}$F]**44** (log $D$ = 3.59 ± 0.02) | | |
| blood | 4.31 ± 0.34 | 3.94 ± 0.46 | 4.45 ± 0.28 | 4.45 ± 0.51 |
| brain | 7.87 ± 0.48 | 4.54 ± 0.37 | 3.38 ± 0.25 | 2.83 ± 0.15 |
| heart | 5.59 ± 0.69 | 3.11 ± 0.81 | 3.33 ± 0.43 | 3.70 ± 0.43 |
| liver | 10.40 ± 0.83 | 5.94 ± 0.97 | 4.28 ± 0.47 | 3.06 ± 0.55 |
| spleen | 4.52 ± 0.46 | 3.29 ± 0.75 | 2.87 ± 0.23 | 2.86 ± 0.51 |
| lung | 5.85 ± 0.68 | 3.02 ± 0.60 | 3.57 ± 0.21 | 2.72 ± 0.59 |
| kidney | 9.57 ± 0.68 | 4.42 ± 0.53 | 3.62 ± 0.19 | 3.45 ± 0.88 |
| stomach[b] | 3.61 ± 0.45 | 5.61 ± 0.81 | 4.63 ± 0.69 | 3.67 ± 1.11 |
| intestine[b] | 12.06 ± 0.35 | 11.15 ± 1.30 | 25.23 ± 3.23 | 19.00 ± 4.14 |
| bone | 2.04 ± 0.33 | 2.43 ± 0.60 | 3.77 ± 0.97 | 6.70 ± 1.21 |

[a]Expressed as % injected dose per gram unless otherwise indicated. Data are the average for five mice ± standard deviation. [b]Expressed as % injected dose per organ.

Table 4. Comparison of Inhibition Constants ($K_i$, nM) and Brain Kinetics between $^{18}$F-Labeled Tracers in This Work and Other Tracers

| compd | $K_i$ (nM) | 2 min[a] | 60 min[a] | $\text{brain}_{2\text{min}}/\text{brain}_{60\text{min}}$ |
|---|---|---|---|---|
| [$^{18}$F]**7**[b] | 6.7 ± 0.3 | 8.14 ± 2.03 | 2.60 ± 0.22 | 3.13 |
| [$^{18}$F]**8**[c] | 2.87 ± 0.17 | 7.33 ± 1.54 | 1.88 ± 0.14 | 3.90 |
| [$^{18}$F]**11**[d] | 2.0 ± 0.5 | 2.88 ± 0.46 | 2.80 ± 0.06 | 1.03 |
| [$^{18}$F]**12**[d] | 3.9 ± 0.2 | 8.18 ± 0.59 | 3.87 ± 0.42 | 2.11 |
| [$^{18}$F]**13**[d] | 1.0 ± 0.2 | 5.16 ± 0.30 | 2.44 ± 0.36 | 2.11 |
| [$^{18}$F]**14**[d] | 2.4 ± 0.1 | 7.38 ± 0.84 | 3.15 ± 0.10 | 2.34 |
| [$^{18}$F]**16**[e] | 9.5 ± 1.3 | 8.12 ± 0.51 | 3.04 ± 0.16 | 2.67 |
| [$^{18}$F]**17**[e] | 3.9 ± 0.2 | 5.29 ± 0.19 | 2.12 ± 0.08 | 2.50 |
| [$^{18}$F]**19**[f] | 2.2 ± 0.5 | 10.27 ± 1.30 | 3.94 ± 0.04 | 2.61 |
| [$^{18}$F]**20**[f] | 3.8 ± 0.5 | 5.53 ± 0.56 | 2.18 ± 0.09 | 2.54 |
| [$^{18}$F]**21**[f] | 4.7 ± 0.9 | 2.57 ± 0.12 | 1.80 ± 0.25 | 1.43 |
| [$^{18}$F]**29** | 76.9 ± 15.5 | 4.05 ± 0.36 | 1.78 ± 0.21 | 2.28 |
| [$^{18}$F]**31** | 9.9 ± 0.5 | 3.79 ± 0.41 | 1.82 ± 0.07 | 2.08 |
| [$^{18}$F]**32** | 8.0 ± 3.2 | 7.23 ± 0.04 | 1.55 ± 0.17 | 4.66 |
| [$^{18}$F]**33** | 2.7 ± 0.7 | 7.27 ± 0.19 | 1.47 ± 0.25 | 4.95 |
| [$^{18}$F]**41** | 9.3 ± 0.1 | 2.23 ± 0.33 | 1.26 ± 0.15 | 1.77 |
| [$^{18}$F]**43** | 5.8 ± 1.8 | 3.26 ± 0.21 | 1.84 ± 0.22 | 1.77 |
| [$^{18}$F]**44** | 10.1 ± 2.4 | 7.87 ± 0.48 | 2.83 ± 0.15 | 2.78 |

[a]Expressed as % injected dose per gram. [b]Data from ref 40. [c]Data from ref 25. [d]Data from ref 30. [e]Data from ref 32. [f]Data from ref 28.


dx.doi.org/10.1021/jm300973k | J. Med. Chem. 2012, 55, 9283−9296

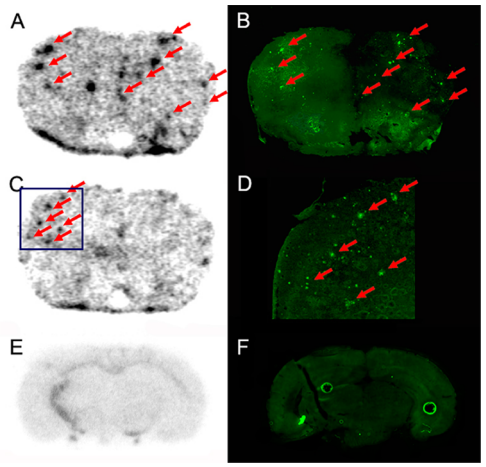


**Figure 6.** Autoradiography of [$^{18}$F]**32** ex vivo using Tg model mouse (C57BL6, APPswe/PSEN1, 10 months old, male) (A, C) and wild-type controls (C57BL6, 10 months old) (E). Plaques were also confirmed by the staining of the same sections with thioflavin S.

and 2,2′-oxidiethanol (5.0 g, 5 mmol) in $CH_2Cl_2$ (200 mL) was added KOH (21.1 g, 40 mmol). The mixture was stirred at 0 °C for 6 h. After reaction, the mixture was washed with water (3 × 100 mL). The organic layer was dried over anhydrous $MgSO_4$. After removal of the solvent, the residue was purified by recrystallization in anhydrous MeOH to give **18** (18.1 g, 92.7%). $^1$H NMR (400 MHz, $CDCl_3$): $\delta$ 7.78 (d, $J$ = 8.3 Hz, 4H), 7.34 (d, $J$ = 8.2 Hz, 4H), 4.09 (t, $J$ = 4.6 Hz, 4H), 3.61 (t, $J$ = 4.7 Hz, 4H), 2.45 (s, 6H).

**(Ethane-1,2-diylbis(oxy))bis(ethane-2,1-diyl) Bis(4-methylbenzenesulfonate) (19).** The same reaction as described above to prepare **18** was used, and **19** was obtained as a white crystal (24.7 g, 71.5%). $^1$H NMR (400 MHz, $CDCl_3$): $\delta$ 7.79 (d, $J$ = 8.3 Hz, 4H), 7.34 (d, $J$ = 8.2 Hz, 4H), 4.14 (t, $J$ = 4.7 Hz, 4H), 3.65 (t, $J$ = 4.9 Hz, 4H), 3.53 (s, 4H), 2.44 (s, 6H).

**2-(2-Fluoroethoxy)ethyl 4-Methylbenzenesulfonate (20).** Intermediate **20** was synthesized according to the literature.[38] Briefly, to a solution of **18** (2.3 g, 5 mmol) in dry THF (30 mL) was added anhydrous TBAF (10 mL, 10 mmol, 1 M in THF). The solution was stirred at 70 °C for 5 h. After removal of solvent, the residue was purified by silica gel chromatography to give **20** (540 mg, 37.1%) as a colorless oil. $^1$H NMR (400 MHz, $CDCl_3$): $\delta$ 7.81 (d, $J$ = 8.2 Hz, 2H), 7.35 (d, $J$ = 8.1 Hz, 2H), 4.58–4.52 (m, 1H), 4.46–4.40 (m, 1H), 4.21–4.16 (m, 2H), 3.75–3.62 (m, 4H), 2.45 (s, 3H).

**2-(2-(2-Fluoroethoxy)ethoxy)ethyl 4-Methylbenzenesulfonate (21).** The same reaction as described above to prepare **20** was used, and **21** was obtained as a colorless oil (309.2 mg, 20.2%). $^1$H NMR (400 MHz, $CDCl_3$): $\delta$ 7.80 (d, $J$ = 8.1 Hz, 2H), 7.34 (d, $J$ = 8.1 Hz, 2H), 4.59 (t, $J$ = 3.8 Hz, 1H), 4.48 (t, $J$ = 3.8 Hz, 1H), 4.17 (t, $J$ = 4.6 Hz, 2H), 3.74 (t, $J$ = 4.2 Hz, 1H), 3.61–3.72 (m, 3H), 3.61 (s, 4H), 2.45 (s, 3H).

**2-Amino-4-methoxyphenol (22).** Intermediate **22** was synthesized according to the literature.[32] Briefly, a mixture of 4-methoxy-2-nitrophenol (3.5 g, 20.7 mmol) and Pd/C (10%, 0.5 g) in absolute methanol (100 mL) under a hydrogen atmosphere (balloon) was vigorously stirred for 24 h at room temperature. The mixture was filtered and the filtrate washed with methanol (20 mL). Evaporation of the solvent under reduced pressure gave **22** as brown flake crystal (2.8 g, 97.3%). Mp: 133.4–135.7 °C.

**5-(5-Methoxybenzo[*d*]oxazol-2-yl)pyridin-2-amine (23).** A solution of **22** (1.0 g, 7 mmol) and 5-(trifluoromethyl)pyridin-2-amine (1.7 g, 10.8 mmol) in NaOH (1 M in water, 20 mL) was stirred at 90 °C for 3 h. After the mixture was cooled to room temperature, the precipitate was collected by filtration. Compound **23** (1.5 g, 88.9%) was obtained as a white solid. Mp: 204.1–205.9 °C. $^1$H NMR (400 MHz, DMSO-$d_6$): $\delta$ 8.71 (d, $J$ = 2.1 Hz, 1H), 8.05 (dd, $J$ = 6.6, 2.2 Hz, 1H), 7.58 (d, $J$ = 8.8 Hz, 1H), 7.25 (d, $J$ = 2.3 Hz, 1H), 6.92 (dd, $J$ = 6.5, 2.4 Hz, 1H), 6.80 (s, 2H), 6.59 (d, $J$ = 8.8 Hz, 1H), 3.81 (s, 3H). MS (ESI): $m/z$ calcd for $C_{13}H_{11}N_3O_2$ 241.09; found 241.9 $(M + H)^+$.

**5-(5-Methoxybenzo[*d*]oxazol-2-yl)-*N*-methylpyridin-2-amine (24).** To a mixture of **23** (480 mg, 2 mmol) and paraformaldehyde (240 mg, 8 mmol) in MeOH (20 mL) was added $CH_3ONa$ (1.08 g, 20 mmol). The mixture was stirred under reflux for 1 h. After the mixture was cooled, $NaBH_4$ (160 mg, 4 mmol) was added, and the mixture was brought to reflux again for 2 h. The reaction mixture was poured onto ice–water, and the precipitate was collected by filtration to obtain **24** as a white solid (500 mg, 98.0%). Mp: 178.6–179.8 °C. $^1$H NMR (400 MHz, DMSO-$d_6$): $\delta$ 8.78 (d, $J$ = 1.9 Hz, 1H), 8.04 (d, $J$ = 8.5 Hz, 1H), 7.59 (d, $J$ = 8.8 Hz, 1H), 7.35 (d, $J$ = 4.5 Hz, 1H), 7.25 (d, $J$ = 2.3 Hz, 1H), 6.91 (dd, $J$ = 6.5, 2.3 Hz, 1H), 6.61 (d, $J$ = 8.9 Hz, 1H), 3.81 (s, 3H), 2.87 (d, $J$ = 4.7 Hz, 3H). MS (ESI): $m/z$ calcd for $C_{14}H_{13}N_3O_2$ 255.1; found 255.9 $(M + H)^+$.

**5-(5-Methoxybenzo[*d*]oxazol-2-yl)-*N*,*N*-dimethylpyridin-2-amine (25).** To a solution of **23** (480 mg, 2 mmol) and paraformaldehyde (300 mg, 10 mmol) in acetic acid (50 mL) was added $NaCNBH_3$ (189 mg, 6 mmol) in one portion at room temperature. The resulting mixture was stirred at room temperature overnight. After neutralization with $NH_4OH$, water was added, and the precipitate was collected by filtration to give **25** as a white solid (481 mg, 89.4%). Mp: 140.0–141.6 °C. $^1$H NMR (400 MHz, DMSO-$d_6$): $\delta$ 8.84 (d, $J$ = 2.1 Hz, 1H), 8.14 (dd, $J$ = 6.9, 2.2 Hz, 1H), 7.59 (d, $J$ = 8.8 Hz, 1H), 7.26 (d, $J$ = 2.3 Hz, 1H), 6.92 (dd, $J$ = 6.4, 2.4 Hz, 1H), 6.80 (d, $J$ = 9.1 Hz, 1H), 3.81 (s, 3H), 3.14 (s, 6H). MS (ESI): $m/z$ calcd for $C_{15}H_{15}N_3O_2$ 269.12, found 270.0 $(M + H)^+$.

**2-(6-(Methylamino)pyridin-3-yl)benzo[*d*]oxazol-5-ol (26).** To a solution of **24** (480 mg, 1.88 mmol) in $CH_2Cl_2$ (30 mL) was added $BBr_3$ (10 mL, 1 M solution in $CH_2Cl_2$) dropwise at −78 °C in a liquid nitrogen–ethanol bath. The mixture was allowed to warm to room temperature and was stirred overnight. Water was added to quench the reaction. After neutralization with $NH_4OH$, the mixture was extracted with $CH_2Cl_2$. The solvent was removed, and **26** was obtained as a white solid (442 mg, 97%). Mp: 237.1–238.6 °C. $^1$H NMR (400 MHz, DMSO-$d_6$): $\delta$ 9.41 (s, 1H), 8.76 (d, $J$ = 1.6 Hz, 1H), 8.02 (dd, $J$ = 7.2, 1.4 Hz, 1H), 7.47 (d, $J$ = 8.7 Hz, 1H), 7.32 (d, $J$ = 4.4 Hz, 1H), 7.00 (d, $J$ = 2.1 Hz, 1H), 6.75 (dd, $J$ = 6.4, 2.2 Hz, 1H), 6.60 (d, $J$ = 8.8 Hz, 1H), 2.87 (d, $J$ = 4.7 Hz, 3H). MS (ESI): $m/z$ calcd for $C_{13}H_{11}N_3O_2$ 241.1, found 241.8 $(M + H)^+$.

**2-(6-(Dimethylamino)pyridin-3-yl)benzo[*d*]oxazol-5-ol (27).** The same reaction as described above to prepare **26** was used, and **27** was obtained as a white solid (348 mg, 88.5%). Mp: 285.2–286.7 °C. $^1$H NMR (400 MHz, DMSO-$d_6$): $\delta$ 9.43 (s, 1H), 8.82 (d, $J$ = 2.1 Hz, 1H), 8.13 (dd, $J$ = 9.0, 2.3 Hz, 1H), 7.48 (d, $J$ = 8.7 Hz, 1H), 7.01 (d, $J$ = 2.2 Hz, 1H), 6.80 (d, $J$ = 9.1 Hz, 1H), 6.76 (dd, $J$ = 8.7, 2.3 Hz, 1H), 3.14 (s, 6H). MS (ESI): $m/z$ calcd for $C_{14}H_{13}N_3O_2$ 255.1, found 255.9 $(M + H)^+$.

**5-(5-(2-(2-Fluoroethoxy)ethoxy)benzo[*d*]oxazol-2-yl)-*N*-methylpyridin-2-amine (28).** A solution of **26** (48 mg, 0.2 mmol), 2-(2-fluoroethoxy)ethyl 4-methylbenzenesulfonate (60 mg, 0.2 mmol), and $K_2CO_3$ (28 mg, 0.2 mmol) in DMF (6 mL) was stirred at 110 °C for 3 h. The aqueous portion was extracted with dichloromethane (3 × 15 mL), and the organic layer was dried over anhydrous $MgSO_4$. $CH_2Cl_2$ was removed in vacuum. The residue was purified by column chromatography (petroleum ether/AcOEt, 1/2) to give **28** as a white solid (41 mg, 62.2%). Mp: 134.8–135.6 °C. $^1$H NMR (400 MHz, $CDCl_3$): $\delta$ 8.92 (s, 1H), 8.21 (dd, $J$ = 7.0, 1.7 Hz, 1H), 7.41 (d, $J$ = 8.8 Hz, 1H), 7.21 (d, $J$ = 2.2 Hz, 1H), 6.93 (dd, $J$ = 6.6, 2.2 Hz, 1H), 6.48 (d, $J$ = 8.8 Hz, 1 H), 5.12 (d, $J$ = 4.4 Hz, 1H), 4.61 (dt, $J$ = 47.6, 4.0 Hz, 2H), 4.19 (t, $J$ = 4.5 Hz, 2H), 3.92 (t, $J$ = 4.8 Hz, 2H), 3.87 (t, $J$ = 4.0 Hz, 1H), 3.80 (t, $J$ = 4.1 Hz, 1H), 3.02 (d, $J$ = 5.1 Hz, 3H). HRMS (EI): $m/z$ calcd for $C_{17}H_{19}N_3O_3F$ 332.1410; found 332.1412 $(M + H)^+$.

**5-(5-(2-(2-(2-Fluoroethoxy)ethoxy)ethoxy)benzo[*d*]oxazol-2-yl)-*N*-methylpyridin-2-amine (29).** The same reaction as described above to prepare **28** was used, and **29** was obtained as a white solid (30 mg, 40.2%). Mp: 87.2–89.1 °C. $^1$H NMR (400 MHz, $CDCl_3$): $\delta$ 8.92 (s, 1H), 8.21 (dd, $J$ = 7.0, 1.8 Hz, 1H), 7.40 (d, $J$ = 8.8 Hz, 1H), 7.21 (d, $J$ = 2.2 Hz, 1H), 6.92 (dd, $J$ = 6.6, 2.2 Hz, 1H), 6.49


dx.doi.org/10.1021/jm300973k | J. Med. Chem. 2012, 55, 9283–9296

(d, $J$ = 8.8 Hz, 1H), 5.12 (d, $J$ = 4.4 Hz, 1H), 4.57 (dt, $J$ = 47.7, 4.0 Hz, 2H), 4.18 (t, $J$ = 4.5 Hz, 2H), 3.90 (t, $J$ = 4.8 Hz, 2H), 3.82−3.72 (m, 6H), 3.80 (t, $J$ = 4.1 Hz, 1H), 3.02 (d, $J$ = 5.0 Hz, 3H). HRMS (EI): $m/z$ calcd for $C_{19}H_{23}N_3O_4F$ 376.1673; found 376.1674 $(M + H)^+$.

**5-(5-(2-(2-Fluoroethoxy)ethoxy)benzo[*d*]oxazol-2-yl)-*N*,*N*-dimethylpyridin-2-amine (30).** The same reaction as described above to prepare **28** was used, and **30** was obtained as a white solid (30 mg, 43.5%). Mp: 88.0−89.7 °C. $^1$H NMR (400 MHz, $CDCl_3$): $\delta$ 8.98 (s, 1H), 8.20 (dd, $J$ = 6.8, 2.2 Hz, 1H), 7.40 (d, $J$ = 8.8 Hz, 1H), 7.21 (d, $J$ = 2.3 Hz, 1H), 6.92 (dd, $J$ = 6.4, 2.4 Hz, 1H), 6.59 (d, $J$ = 9.0 Hz, 1H), 4.61 (dt, $J$ = 47.7, 4.1 Hz, 2H), 4.19 (t, $J$ = 4.5 Hz, 2H), 3.92 (t, $J$ = 4.9 Hz, 2H), 3.88 (t, $J$ = 4.2 Hz, 1H), 3.80 (t, $J$ = 4.2 Hz, 1H), 3.19 (s, 6H). HRMS (EI): $m/z$ calcd for $C_{18}H_{21}N_3O_3F$ 346.1567; found 346.1559 $(M + H)^+$.

**5-(5-(2-(2-(2-Fluoroethoxy)ethoxy)ethoxy)benzo[*d*]oxazol-2-yl)-*N*,*N*-dimethylpyridin-2-amine (31).** The same reaction as described above to prepare **28** was used, and **31** was obtained as a white solid (40 mg, 50%). Mp: 120.0−121.8 °C. $^1$H NMR (400 MHz, $CDCl_3$): $\delta$ 8.98 (s, 1H), 8.19 (d, $J$ = 8.9 Hz, 1H), 7.39 (d, $J$ = 8.8 Hz, 1H), 7.27 (d, $J$ = 0.9 Hz, 1H), 6.91 (d, $J$ = 8.6 Hz, 1H), 6.59 (d, $J$ = 9.0 Hz, 1H), 4.50−4.63 (m, 2H), 4.18 (t, $J$ = 4.1 Hz, 2H), 3.90 (t, $J$ = 4.0 Hz, 2H), 3.62−3.82 (m, 6H), 3.19 (s, 6H). HRMS (EI): $m/z$ calcd for $C_{20}H_{25}N_3O_4F$ 390.1829; found 390.1829 $(M + H)^+$.

**5-(5-(2-Fluoroethoxy)benzo[*d*]oxazol-2-yl)-*N*-methylpyridin-2-amine (32).** The same reaction as described above to prepare **28** was used, and **32** was obtained as a white solid (30 mg, 52.5%). Mp: 212.2−212.8 °C. $^1$H NMR (400 MHz, DMSO-$d_6$): $\delta$ 8.78 (d, $J$ = 1.9 Hz, 1H), 8.04 (d, $J$ = 7.5 Hz, 1H), 7.60 (d, $J$ = 8.8 Hz, 1H), 7.36 (d, $J$ = 4.5 Hz, 1H), 7.30 (d, $J$ = 2.3 Hz, 1H), 6.95 (dd, $J$ = 6.4, 2.4 Hz, 1H), 6.61 (d, $J$ = 8.9 Hz, 1 H), 4.77 (dt, $J$ = 47.8, 3.5 Hz, 2H), 4.33 (t, $J$ = 3.7 Hz, 1H), 4.25 (t, $J$ = 3.8 Hz, 1H), 2.87 (d, $J$ = 4.7 Hz, 3H). HRMS (EI): $m/z$ calcd for $C_{15}H_{15}N_3O_2F$ 288.1148; found 288.1147 $(M + H)^+$.

**5-(5-(2-Fluoroethoxy)benzo[*d*]oxazol-2-yl)-*N*,*N*-dimethylpyridin-2-amine (33).** The same reaction as described above to prepare **28** was used, and **33** was obtained as a white solid (54 mg, 89.7%). Mp: 167.0−168.4 °C. $^1$H NMR (400 MHz, $CDCl_3$): $\delta$ 8.98 (s, 1H), 8.20 (d, $J$ = 8.0 Hz, 1H), 7.42 (d, $J$ = 8.4 Hz, 1H), 7.21 (s, 1H), 6.93 (d, $J$ = 7.5 Hz, 1H), 6.60 (d, $J$ = 8.4 Hz, 1H), 4.85 (s, 1H), 4.73 (s, 1H), 4.30 (s, 1H), 4.23 (s, 1H), 3.20 (s, 6H). HRMS (EI): $m/z$ calcd for $C_{16}H_{17}N_3O_2F$ 302.1305; found 302.1307 $(M + H)^+$.

**2-Amino-5-methoxybenzenethiol (34).** Intermediate **34** was synthesized according to the literature.[14] Briefly, a mixture of 6-methoxybenzo[$d$]thiazol-2-amine (9 g, 50 mmol) and KOH (28 g, 500 mmol) in $H_2O$ (100 mL) was stirred at 120 °C overnight. After removal of the scraps by filtering, the filtrate was neutralized by acetic acid (30% in water), and the precipitate was collected by filtration to give **34** (7.75 g, 88.9%) as a light yellow solid. Mp: 81.6−82.8 °C.

**5-(6-Methoxybenzo[*d*]thiazol-2-yl)pyridin-2-amine (35).** The same reaction as described above to prepare **23** was used, and **35** was obtained (1.29 g, 50.2%). Mp: 224.7−225.4 °C. $^1$H NMR (400 MHz, DMSO-$d_6$): $\delta$ 8.58 (s, 1H), 7.98 (d, $J$ = 8.2 Hz, 1H), 7.84 (d, $J$ = 8.8 Hz, 1H), 7.65 (s, 1H), 7.08 (d, $J$ = 8.2 Hz, 1H), 6.70 (s, 2H), 6.57 (d, $J$ = 8.5 Hz, 1H), 3.84 (s, 3H). MS (ESI): $m/z$ calcd for $C_{13}H_{11}N_3OS$ 257.1; found 257.5 $(M + H)^+$.

**5-(6-Methoxybenzo[*d*]thiazol-2-yl)-*N*-methylpyridin-2-amine (36).** The same reaction as described above to prepare **24** was used, and **36** was obtained as a white solid (798 mg, 98%). Mp: 194.7−195.6 °C. $^1$H NMR (400 MHz, DMSO-$d_6$): $\delta$ 8.64 (s, 1H), 7.96 (d, $J$ = 7.4 Hz, 1H), 7.83 (d, $J$ = 8.8 Hz, 1H), 7.64 (d, $J$ = 1.6 Hz, 1H), 7.20 (d, $J$ = 4.6 Hz, 1H), 7.07 (dd, $J$ = 6.8, 2.1 Hz, 1H), 6.57 (d, $J$ = 8.8 Hz, 1H), 3.84 (s, 3H), 2.86 (d, $J$ = 4.6 Hz, 3H). MS (ESI): $m/z$ calcd for $C_{14}H_{13}N_3OS$ 271.1, found 271.8 $(M + H)^+$.

**5-(6-Methoxybenzo[*d*]thiazol-2-yl)-*N*,*N*-dimethylpyridin-2-amine (37).** The same reaction as described above to prepare **25** was used, and **37** was obtained (0.65 g, 91.1%). Mp: 175.4−176.7 °C. $^1$H NMR (400 MHz, $CDCl_3$): $\delta$ 8.76 (d, $J$ = 2.3 Hz, 1H), 8.13 (dd, $J$ = 9.0, 2.3 Hz, 1H), 7.87 (d, $J$ = 8.9 Hz, 1H), 7.32 (d, $J$ = 2.4 Hz, 1H), 7.05 (dd, $J$ = 8.9, 2.4 Hz, 1H), 6.58 (d, $J$ = 9.0 Hz, 1H), 3.88 (s, 3H), 3.18 (s, 6H). MS (ESI): $m/z$ calcd for $C_{15}H_{15}N_3OS$ 285.1; found 285.6 $(M + H)^+$.

**2-(6-(Methylamino)pyridin-3-yl)benzo[*d*]thiazol-6-ol (38).** The same reaction as described above to prepare **26** was used, and **38** was obtained as a white solid (653 mg, 88.4%). Mp: 238.5−244.2 °C. $^1$H NMR (400 MHz, DMSO-$d_6$): $\delta$ 9.72 (s, 1H), 8.61 (s, 1H), 7.94 (d, $J$ = 8.3 Hz, 1H), 7.74 (d, $J$ = 8.6 Hz, 1H), 7.36 (s, 1H), 7.17 (d, $J$ = 3.8 Hz, 1H), 6.93 (d, $J$ = 6.8 Hz, 1H), 6.57 (d, $J$ = 8.7 Hz, 1H), 2.86 (d, $J$ = 4.2 Hz, 3H). MS (ESI): $m/z$ calcd for $C_{13}H_{11}N_3OS$ 257.1, found 257.9 $(M + H)^+$.

**2-(6-(Dimethylamino)pyridin-3-yl)benzo[*d*]thiazol-6-ol (39).** The same reaction as described above to prepare **26** was used, and **39** was obtained as a white solid (0.61 g, 68.2%). Mp: 287.2−288.7 °C. $^1$H NMR (400 MHz, DMSO-$d_6$): $\delta$ 9.74 (s, 1H), 8.68 (d, $J$ = 2.1 Hz, 1H), 8.04 (dd, $J$ = 9.0, 2.2 Hz, 1H), 7.75 (d, $J$ = 8.7 Hz, 1H), 7.36 (d, $J$ = 2.1 Hz, 1H), 6.94 (dd, $J$ = 8.7, 2.1 Hz, 1H), 6.76 (d, $J$ = 9.0 Hz, 1H), 3.12 (s, 6H). MS (ESI): $m/z$ calcd for $C_{14}H_{13}N_3OS$ 271.1; found 271.5 $(M + H)^+$.

**5-(6-(2-(2-Fluoroethoxy)ethoxy)benzo[*d*]thiazol-2-yl)-*N*-methylpyridin-2-amine (40).** The same reaction as described above to prepare **28** was used, and **40** was obtained as a white solid (40 mg, 55.2%). Mp: 155.7−157.5 °C. $^1$H NMR (400 MHz, $CDCl_3$): $\delta$ 8.72 (d, $J$ = 2.0 Hz, 1H), 8.10 (dd, $J$ = 6.5, 2.2 Hz, 1H), 7.86 (d, $J$ = 8.9 Hz, 1H), 7.35 (d, $J$ = 2.3 Hz, 1H), 7.08 (dd, $J$ = 6.5, 2.4 Hz, 1H), 6.46 (d, $J$ = 8.8 Hz, 1H), 4.98 (d, $J$ = 4.6 Hz, 1H), 4.61 (dt, $J$ = 47.6, 4.0 Hz, 2H), 4.21 (t, $J$ = 4.5 Hz, 2H), 3.93 (t, $J$ = 4.9 Hz, 2H), 3.87 (t, $J$ = 4.1 Hz, 1H), 3.80 (t, $J$ = 4.2 Hz, 1H), 2.99 (d, $J$ = 5.1 Hz, 3H). HRMS (EI): $m/z$ calcd for $C_{17}H_{19}N_3O_2FS$ 348.1182; found 348.1179 $(M + H)^+$.

**5-(6-(2-(2-(2-Fluoroethoxy)ethoxy)ethoxy)benzo[*d*]thiazol-2-yl)-*N*-methylpyridin-2-amine (41).** The same reaction as described above to prepare **28** was used, and **41** was obtained as a white solid (45 mg, 57.3%). Mp: 126.4−128.7 °C. $^1$H NMR (400 MHz, $CDCl_3$): $\delta$ 8.71 (d, $J$ = 2.0 Hz, 1H), 8.10 (dd, $J$ = 6.5, 2.2 Hz, 1H), 7.86 (d, $J$ = 8.9 Hz, 1H), 7.34 (d, $J$ = 2.3 Hz, 1H), 7.08 (dd, $J$ = 6.5, 2.4 Hz, 1H), 6.46 (d, $J$ = 8.8 Hz, 1H), 4.98 (d, $J$ = 4.6 Hz, 1H), 4.57 (dt, $J$ = 47.7, 4.0 Hz, 2H), 4.20 (t, $J$ = 4.6 Hz, 2H), 3.90 (t, $J$ = 4.9 Hz, 2H), 3.69−3.81 (m, 6H), 2.99 (d, $J$ = 5.1 Hz, 3H). HRMS (EI): $m/z$ calcd for $C_{19}H_{23}N_3O_3FS$ 392.1444; found 392.1446 $(M + H)^+$.

**5-(6-(2-(2-Fluoroethoxy)ethoxy)benzo[*d*]thiazol-2-yl)-*N*,*N*-dimethylpyridin-2-amine (42).** The same reaction as described above to prepare **28** was used, and **42** was obtained as a white solid (50 mg, 75%). Mp: 140.3−141.1 °C. $^1$H NMR (400 MHz, $CDCl_3$): $\delta$ 8.76 (s, 1H), 8.12 (dd, $J$ = 6.6, 2.3 Hz, 1H), 7.86 (d, $J$ = 8.9 Hz, 1H), 7.34 (d, $J$ = 2.4 Hz, 1H), 7.07 (dd, $J$ = 6.5, 2.4 Hz, 1H), 6.57 (d, $J$ = 9.0 Hz, 1H), 4.60 (dt, $J$ = 47.7, 4.0 Hz, 2H), 4.21 (t, $J$ = 4.5 Hz, 2H), 3.93 (t, $J$ = 4.9 Hz, 2H), 3.87 (t, $J$ = 4.2 Hz, 1H), 3.80 (t, $J$ = 4.1 Hz, 1H), 3.10 (s, 6H). HRMS (EI): $m/z$ calcd for $C_{18}H_{21}N_3O_2FS$ 362.1339; found 362.1338 $(M + H)^+$.

**5-(6-(2-(2-(2-Fluoroethoxy)ethoxy)ethoxy)benzo[*d*]thiazol-2-yl)-*N*,*N*-dimethylpyridin-2-amine (43).** The same reaction as described above to prepare **28** was used, and **43** was obtained as a white solid (32.4 mg, 40%). Mp: 109.9−111.3 °C. $^1$H NMR (400 MHz, $CDCl_3$): $\delta$ 8.76(s, 1H), 8.11 (dd, $J$ = 6.6, 2.4 Hz, 1H), 7.85 (d, $J$ = 8.9 Hz, 1H), 7.34 (d, $J$ = 2.3 Hz, 1H), 7.07 (dd, $J$ = 6.5, 2.4 Hz, 1H), 6.57 (d, $J$ = 9.0 Hz, 1H), 4.56 (dt, $J$ = 47.7, 4.0 Hz, 2H), 4.20 (t, $J$ = 4.6 Hz, 2H), 3.90 (t, $J$ = 4.9 Hz, 2H), 3.71−3.81 (m, 6H), 3.17 (s, 6H). HRMS (EI): $m/z$ calcd for $C_{20}H_{25}N_3O_3FS$ 406.1601; found 406.1590 $(M + H)^+$.

**5-(6-(2-Fluoroethoxy)benzo[*d*]thiazol-2-yl)-*N*-methylpyridin-2-amine (44).** The same reaction as described above to prepare **28** was used, and **44** was obtained as a white solid (40 mg, 64.6%). Mp: 182.8−184.6 °C. $^1$H NMR (400 MHz, $CDCl_3$): $\delta$ 8.72 (d, $J$ = 2.0 Hz, 1H), 8.11 (dd, $J$ = 6.5, 2.3 Hz, 1H), 7.88 (d, $J$ = 8.9 Hz, 1H), 7.36 (d, $J$ = 2.4 Hz, 1H), 7.09 (dd, $J$ = 6.4, 2.4 Hz, 1H), 6.47 (d, $J$ = 8.8 Hz, 1H), 4.80 (dt, $J$ = 47.4, 4.0 Hz, 2H), 4.32 (t, $J$ = 4.2 Hz, 1H), 4.25 (t, $J$ = 4.2 Hz, 1H), 3.00 (d, $J$ = 5.1 Hz, 3H). HRMS (EI): $m/z$ calcd for $C_{15}H_{15}N_3OFS$ 304.0920; found 304.0924 $(M + H)^+$.

**5-(6-(2-Fluoroethoxy)benzo[*d*]thiazol-2-yl)-*N*,*N*-dimethylpyridin-2-amine (45).** The same reaction as described above to


dx.doi.org/10.1021/jm300973k | J. Med. Chem. 2012, 55, 9283−9296

prepare **28** was used, and **45** was obtained as a white solid (30 mg, 78.9%). Mp: 166.1−168.5 °C. $^1$H NMR (400 MHz, $CDCl_3$): $\delta$ 8.69 (d, $J$ = 2.3 Hz, 1H), 8.05 (dd, $J$ = 6.6, 2.4 Hz, 1H), 7.80 (d, $J$ = 8.9 Hz, 1H), 7.28 (d, $J$ = 2.4 Hz, 1H), 7.01 (dd, $J$ = 6.4, 2.4 Hz, 1H), 6.51 (d, $J$ = 9.0 Hz, 1H), 4.72 (dt, $J$ = 47.4, 4.0 Hz, 2H), 4.24 (t, $J$ = 4.2 Hz, 1H), 4.17 (t, $J$ = 4.2 Hz, 1H), 3.10 (s, 6H). HRMS (EI): $m/z$ calcd for $C_{16}H_{17}N_3OFS$ 318.1076; found 318.1075 $(M + H)^+$.

**2-(2-(6-(Dimethylamino)pyridin-3-yl)benzo[*d*]oxazol-5-yloxy)ethyl 4-Methylbenzenesulfonate (46).** To a solution of **27** (60 mg, 0.24 mmol) in acetone (30 mL) was added ethane-1,2-diyl bis(4-methylbenzenesulfonate) (131 mg, 0.35 mmol), $K_2CO_3$ (124 mg, 0.9 mmol), and 18-crown-6 in catalytic amount. The mixture was stirred at 75 °C for 3 h. Acetone was removed in vacuum. The residue was purified by column chromatography (petroleum ether/AcOEt, 1/1) to give **46** as a white solid (38.5 mg, 35.4%). Mp: 179.1−179.5 °C. $^1$H NMR (400 MHz, $CDCl_3$): $\delta$ 8.97 (s, 1H), 8.19 (d, $J$ = 8.9 Hz, 1H), 7.83 (d, $J$ = 8.3 Hz, 2H), 7.37 (d, $J$ = 8.8 Hz, 1H), 7.34 (d, $J$ = 8.1 Hz, 2H), 7.06 (d, $J$ = 2.4 Hz, 1H), 6.77 (dd, $J$ = 8.8, 2.5 Hz, 1H), 6.60 (d, $J$ = 9.0 Hz, 1 H), 4.17−4.42 (m, 4H), 3.21 (s, 6H), 2.44 (s, 3H). MS (ESI): $m/z$ calcd for $C_{23}H_{23}N_3O_5S$ 453.14, found 454.11 $(M + H)^+$.

**2-(2-(2-(2-(6-(Dimethylamino)pyridin-3-yl)benzo[*d*]oxazol-5-yloxy)ethoxy)ethoxy)ethyl 4-Methylbenzenesulfonate (47).** The same reaction as described above to prepare **46** was used, and **47** was obtained as a white solid (60 mg, 27.7%). Mp: 86.3−87.9 °C. $^1$H NMR (400 MHz, $CDCl_3$): $\delta$ 8.98(s, 1H), 8.22 (d, $J$ = 7.7 Hz, 1H), 7.79 (d, $J$ = 8.2 Hz, 2H), 7.40 (d, $J$ = 8.8 Hz, 1H), 7.32 (d, $J$ = 8.1 Hz, 2H), 7.20 (d, $J$ = 2.4 Hz, 1H), 6.91 (dd, $J$ = 6.6, 2.2 Hz, 1H), 6.62 (d, $J$ = 8.5 Hz, 1H), 4.16 (m, 4H), 3.85 (t, $J$ = 4.9 Hz, 2H), 3.61−3.73 (m, 6H), 3.22 (s, 6H), 2.42 (s, 3H). MS (ESI): $m/z$ calcd for $C_{27}H_{31}N_3O_7S$ 541.2, found 542.0 $(M + H)^+$.

**2-(2-(6-(Methylamino)pyridin-3-yl)benzo[*d*]oxazol-5-yloxy)-ethyl 4-Methylbenzenesulfonate (48).** The same reaction as described above to prepare **46** was used, and **48** was obtained as a white solid (40 mg, 30.5%). Mp: 169.7−170.7 °C. $^1$H NMR (400 MHz, $CDCl_3$): $\delta$ 8.90 (s, 1H), 8.22 (dd, $J$ = 8.8, 2.0 Hz, 1H), 7.83 (d, $J$ = 8.2 Hz, 2H), 7.38 (d, $J$ = 8.8 Hz, 1H), 7.34 (d, $J$ = 8.1 Hz, 2H), 7.07 (d, $J$ = 2.4 Hz, 1H), 6.78 (dd, $J$ = 8.8, 2.4 Hz, 1H), 6.51 (d, $J$ = 8.8 Hz, 1 H), 5.37 (s, 1H), 4.40 (t, $J$ = 4.4 Hz, 2H), 4.18 (t, $J$ = 5.0 Hz, 2H), 3.02 (d, $J$ = 5.0 Hz, 3H), 2.44 (s, 3H). MS (ESI): $m/z$ calcd for $C_{22}H_{21}N_3O_5S$ 439.12, found 440.09 $(M + H)^+$.

**2-(2-(2-(2-(6-(Methylamino)pyridin-3-yl)benzo[*d*]oxazol-5-yloxy)ethoxy)ethoxy)ethyl 4-Methylbenzenesulfonate (49).** The same reaction as described above to prepare **46** was used, and **49** was obtained as a white solid (75 mg, 47.8%). Mp: 91.3 − 92.2 °C. $^1$H NMR (400 MHz, $CDCl_3$): $\delta$ 8.90 (d, $J$ = 2.0 Hz, 1H), 8.16 (dd, $J$ = 6.7, 2.1 Hz, 1H), 7.77 (d, $J$ = 8.2 Hz, 2H), 7.37 (d, $J$ = 8.8 Hz, 1H), 7.29 (d, $J$ = 8.1 Hz, 2H), 7.17 (d, $J$ = 2.4 Hz, 1H), 6.88 (dd, $J$ = 6.4, 2.4 Hz, 1H), 6.45 (d, $J$ = 8.8 Hz, 1H), 5.25 (d, $J$ = 4.8 Hz, 1H), 4.11−4.17 (m, 4H), 3.82 (t, $J$ = 4.9 Hz, 2H), 3.59−3.70 (m, 6H), 2.98 (d, $J$ = 5.1 Hz, 3H), 2.39 (s, 3H). MS (ESI): $m/z$ calcd for $C_{26}H_{29}N_3O_7S$ 527.17, found 528.19 $(M + H)^+$.

**2-(2-(6-(*tert*-Butoxycarbonyl)pyridin-3-yl)benzo[*d*]oxazol-5-yloxy)ethyl 4-Methylbenzenesulfonate (50).** To a solution of **48** (40 mg, 0.09 mmol) in THF (30 mL) was added excessive $(Boc)_2O$. The mixture was stirred at 85 °C for 28 h. After solvent was removed in vacuum, the residue was purified by column chromatography (petroleum ether/AcOEt, 1/1) to give **50** as a white solid (32.7 mg, 66.7%). Mp: 172.1−173.2 °C. $^1$H NMR (400 MHz, $CDCl_3$): $\delta$ 9.16 (s, 1H), 8.37 (dd, $J$ = 8.9, 6.6 Hz, 1H), 8.02 (d, $J$ = 8.8 Hz, 1H), 7.83 (d, $J$ = 8.3 Hz, 2H), 7.44 (d, $J$ = 8.9 Hz, 1H), 7.35 (d, $J$ = 8.0 Hz, 2H), 7.12 (d, $J$ = 2.4 Hz, 1H), 6.86 (dd, $J$ = 8.9, 2.5 Hz, 1H), 4.19−4.43 (m, 4H), 3.51 (s, 3H), 2.45 (s, 3H), 1.57 (s, 9H). MS (ESI): $m/z$ calcd for $C_{27}H_{29}N_3O_7S$ 539.17, found 540.18 $(M + H)^+$.

**2-(2-(2-(2-(6-(*tert*-Butoxycarbonyl)pyridin-3-yl)benzo[*d*]-oxazol-5-yloxy)ethoxy)ethoxy)ethyl 4-Methylbenzenesulfonate (51).** The same reaction as described above to prepare **50** was used, and **51** was obtained as a white solid (20 mg, 22.5%). Mp: 85.0−85.5 °C. $^1$H NMR (400 MHz, $CDCl_3$): $\delta$ 9.16 (s, 1H), 8.37 (dd, $J$ = 6.8, 2.0 Hz, 1H), 7.99 (d, $J$ = 8.9 Hz, 1H), 7.79 (d, $J$ = 8.0 Hz, 2H), 7.45 (d, $J$ = 8.8 Hz, 1H), 7.32 (d, $J$ = 8.0 Hz, 2H), 7.24 (d, $J$ = 2.0 Hz, 1H), 6.98 (dd, $J$ = 6.7, 2.2 Hz, 1H), 4.15−4.19 (m, 4H), 3.86 (t, $J$ = 4.8 Hz, 2H), 3.67−3.69 (m, 4H), 3.63 (t, $J$ = 5.2 Hz, 2H), 3.49 (s, 3H), 2.42 (s, 3H), 1.56 (s, 9H). MS (ESI): $m/z$ calcd for $C_{31}H_{37}N_3O_9S$ 627.23, found 628.0 $(M + H)^+$.

**2-(2-(2-(2-(6-(Dimethylamino)pyridin-3-yl)benzo[*d*]thiazol-6-yloxy)ethoxy)ethoxy)ethyl 4-Methylbenzenesulfonate (52).** The same reaction as described above to prepare **46** was used, and **52** was obtained as a white solid (87 mg, 48.7%). Mp: 107.6−108.7 °C. $^1$H NMR (400 MHz, $CDCl_3$): $\delta$ 8.76 (d, $J$ = 2.2 Hz, 1H), 8.12 (dd, $J$ = 6.6, 2.4 Hz, 1H), 7.85 (d, $J$ = 8.9 Hz, 1H), 7.79 (d, $J$ = 8.2 Hz, 2H), 7.30−7.34 (m, 3H), 7.05 (dd, $J$ = 6.4, 2.5 Hz, 1H), 6.58 (d, $J$ = 9.0 Hz, 1H), 4.15−4.18 (m, 4H), 3.86 (t, $J$ = 4.8 Hz, 2H), 3.61−3.72 (m, 6H), 3.17 (s, 6H), 2.42 (s, 3H). MS(ESI): $m/z$ calcd for $C_{27}H_{31}N_3O_6S_2$ 557.17, found 558.0 $(M + H)^+$.

**2-(2-(2-(Methylamino)pyridin-3-yl)benzo[*d*]thiazol-6-yloxy)-ethyl 4-Methylbenzenesulfonate (53).** The same reaction as described above to prepare **46** was used, and **53** was obtained as a white solid (55 mg, 40.3%). Mp: 153.0−155.4 °C. $^1$H NMR (400 MHz, $CDCl_3$): $\delta$ 8.70 (s, 1H), 8.11 (dd, $J$ = 8.8, 2.3 Hz, 1H), 7.81−7.85 (m, 3H), 7.33 (d, $J$ = 8.0 Hz, 2H), 7.20 (d, $J$ = 2.5 Hz, 1H), 6.92 (dd, $J$ = 8.9, 2.6 Hz, 1H), 6.47 (d, $J$ = 8.8 Hz, 1H), 5.02 (d, $J$ = 4.5 Hz, 1H), 4.20−4.43 (m, 4H), 3.01 (d, $J$ = 5.2 Hz, 3H), 2.44 (s, 3H). MS (ESI): $m/z$ calcd for $C_{22}H_{21}N_3O_4S_2$ 455.1, found 456.06 $(M + H)^+$.

**2-(2-(2-(2-(6-(Methylamino)pyridin-3-yl)benzo[*d*]thiazol-6-yloxy)ethoxy)ethoxy)ethyl 4-Methylbenzenesulfonate (54).** The same reaction as described above to prepare **46** was used, and **54** was obtained as a white solid (63 mg, 38.4%). Mp: 110.1−110.9 °C. $^1$H NMR (400 MHz, $CDCl_3$): $\delta$ 8.71 (d, $J$ = 2.2 Hz, 1H), 8.10 (dd, $J$ = 6.4, 2.3 Hz, 1H), 7.86 (d, $J$ = 8.9 Hz, 1H), 7.79 (d, $J$ = 8.2 Hz, 2H), 7.30−7.35 (m, 3H), 7.06 (dd, $J$ = 6.4, 2.5 Hz, 1H), 6.46 (d, $J$ = 8.8 Hz, 1H), 4.98 (d, $J$ = 4.6 Hz, 1H), 4.15−4.20 (m, 4H), 3.86 (t, $J$ = 4.9 Hz, 2H), 3.63−3.72 (m, 4H), 3.61 (t, $J$ = 3.7 Hz, 2H), 3.00 (d, $J$ = 5.1 Hz, 3H), 2.42 (s, 3H). MS (ESI): $m/z$ calcd for $C_{26}H_{29}N_3O_6S_2$ 543.15, found 543.9 $(M + H)^+$.

**2-(2-(6-(*tert*-Butoxycarbonyl)pyridin-3-yl)benzo[*d*]thiazol-6-yloxy)ethyl 4-Methylbenzenesulfonate (55).** The same reaction as described above to prepare **50** was used, and **55** was obtained as a white solid (53 mg, 79.6%). Mp: 163.4−165.4 °C. $^1$H NMR (400 MHz, $CDCl_3$): $\delta$ 8.97 (d, $J$ = 2.2 Hz, 1H), 8.27 (dd, $J$ = 8.8, 2.4 Hz, 1H), 7.92 (dd, $J$ = 8.8, 7.2 Hz, 2H), 7.82 (d, $J$ = 8.3 Hz, 2H), 7.34 (d, $J$ = 8.1 Hz, 2H), 7.25 (d, $J$ = 2.6 Hz, 1H), 6.98 (dd, $J$ = 9.0, 2.6 Hz, 1H), 4.22−4.44 (m, 4H), 3.48 (s, 3H), 2.44 (s, 3H), 1.56 (s, 9H). MS (ESI): $m/z$ calcd for $C_{27}H_{29}N_3O_6S_2$ 555.15, found 556.13 $(M + H)^+$.

**2-(2-(2-(2-(6-(*tert*-Butoxycarbonyl)pyridin-3-yl)benzo[*d*]-thiazol-6-yloxy)ethoxy)ethoxy)ethyl 4-Methylbenzenesulfonate (56).** The same reaction as described above to prepare **50** was used, and **56** was obtained as a white solid (45 mg, 63.4%). Mp: 88.2−90.1 °C. $^1$H NMR(400 MHz, $CDCl_3$): $\delta$ 8.96 (s, 1H), 8.25 (dd, $J$ = 6.4, 2.4 Hz, 1H), 7.92 (t, $J$ = 8.7 Hz, 2H), 7.79 (d, $J$ = 8.2 Hz, 2H), 7.34 (d, $J$ = 2.5 Hz, 1H), 7.31 (d, $J$ = 8.1 Hz, 2H), 7.11 (dd, $J$ = 6.6, 2.3 Hz, 1H), 4.15−4.22 (m, 4H), 3.87 (t, $J$ = 4.7 Hz, 2H), 3.62−3.73 (m, 6H), 3.47 (s, 3H), 2.42 (s, 3H), 1.56 (s, 9H). MS (ESI): $m/z$ calcd for $C_{31}H_{37}N_3O_8S_2$ 643.20, found 644.18 $(M + H)^+$.

**Radiolabeling.** [$^{18}$F]Fluoride trapped on a QMA cartridge was eluted with 1 mL of (Kryptofix 222)/$K_2CO_3$ solution (13 mg of Kryptofix 222 and 1.1 mg of $K_2CO_3$ in $CH_3CN/H_2O$, 0.8:0.2). The solvent was removed at 120 °C under a stream of nitrogen gas. The residue was azeotropically dried with 1 mL of anhydrous acetonitrile three times at 120 °C under a stream of nitrogen gas.

For [$^{18}$F]**29**, [$^{18}$F]**32**, [$^{18}$F]**41**, and [$^{18}$F]**44**, a solution of the tosylate precursors **51**, **50**, **56**, and **55** (1.0 mg) in $CH_3CN$ (0.5 mL) was added to the reaction vessel containing the $^{18}F^-$ activity, respectively. The mixture was heated at 100 °C for 5 min. After the solution was cooled to room temperature, HCl (1 M aqueous solution, 0.2 mL) was added and the mixture was heated at 100 °C again for 5 min. An aqueous solution of $NaHCO_3$ was added to adjust to pH 8−9. Water (10 mL) was added, and the mixture was passed through a Sep-Pak C18 cartridge (Waters). The cartridge was washed with 10 mL of water, and the labeled compound was eluted with 2 mL of acetonitrile. After the solvent was removed, the residue was dissolved in $CH_3CN$


dx.doi.org/10.1021/jm300973k | J. Med. Chem. 2012, 55, 9283−9296

and subjected to HPLC for purification (Agela Technologies, 5 $\mu$m, 10 mm × 250 mm, $CH_3CN$/water = 6/4; flow rate = 4 mL/min). The retention times of [$^{18}$F]**29**, [$^{18}$F]**32**, [$^{18}$F]**41**, and [$^{18}$F]**44** were 7.72, 6.36, 5.28, and 7.81 min, respectively, in this HPLC system. The preparation took 60 min, and the radiochemical yield was 20−30% (decay not corrected). The radiochemical purity of all tracers was greater than 98%.

For [$^{18}$F]**31**, [$^{18}$F]**33**, and [$^{18}$F]**43**, a solution of the tosylate precursors **47**, **46**, and **52** (1.0 mg) in $CH_3CN$ (0.5 mL) was added to the reaction vessel containing the $^{18}F^-$ activity, respectively. The mixture was heated at 100 °C for 5 min. Water (10 mL) was added, and the mixture was passed through a Sep-Pak C18 cartridge (Waters). The cartridge was washed with 10 mL of water, and the labeled compound was eluted with 2 mL of acetonitrile. The eluted compound was purified by HPLC (Agela Technologies, 5 $\mu$m, 10 mm × 250 mm). The retention times of [$^{18}$F]**31**, [$^{18}$F]**33**, and [$^{18}$F]**43** were 9.09, 5.93, and 8.23 min, respectively, in this HPLC system ($CH_3CN$/water = 7/3; flow rate = 4 mL/min). The preparation took 40 min, and the radiochemical yield was 40−50% (decay not corrected). The radiochemical purity of all tracers was greater than 98%. Specific activity, estimated by comparing the UV peak intensity of purified $^{18}$F-labeled compounds with reference nonradioactive compounds, was approximately 200 GBq/$\mu$mol.

**Binding Assay Using A$\beta_{1-42}$ Aggregates.** Inhibition experiments were carried out in 12 mm × 75 mm borosilicate glass tubes according to procedures described previously with some modifications. The radioligand [$^{125}$I]IMPY was prepared according to procedures described previously.[12] After HPLC purification, the radiochemical purity was greater than 95%. The reaction mixture contained 100 $\mu$L of aggregated A$\beta_{1-42}$ fibrils, 100 $\mu$L of radioligands ([$^{125}$I]IMPY, 60000−100000 cpm/100 $\mu$L), 100 $\mu$L of inhibitors ($10^{-4}$−$10^{-8.5}$ M in ethanol), and 700 $\mu$L of 0.05% bovine serum albumin solution in a final volume of 1 mL. The mixture was incubated at 37 °C for 2 h, and the free radioactivity was separated by vacuum filtration through Whatman GF/B filters using a Brandel Mp-48T cell harvester followed by 3 × 4 mL washes with PBS (0.02 M, pH 7.4) at room temperature. Filters with the bound [$^{125}$I]IMPY were counted in a $\gamma$ counter (WALLAC/Wizard 1470, U.S.) with 70% efficiency. Inhibition experiments were repeated three times, and the half maximal inhibitory concentration ($IC_{50}$) was determined using GraphPad Prism 4.0, and the inhibition constant ($K_i$) was calculated using the Cheng−Prusoff equation:[39] $K_i = IC_{50}/(1 + [L]/K_d)$.

**Partition Coefficient Determination.** The determination of partition coefficients of radiofluorinated tracers was performed according to the procedure previously reported.[32] A solution of $^{18}$F-labeled tracer (1.5 MBq) was added to premixed suspensions containing 3.0 g of *n*-octanol and 3.0 g of PBS (0.05 M, pH 7.4) in a test tube. The test tube was vortexed for 3 min at room temperature, followed by centrifugation for 5 min at 3000 rpm. Two samples from the *n*-octanol (50 $\mu$L) and water (500 $\mu$L) layers were measured. The partition coefficient was expressed as the logarithm of the ratio of the count per gram from *n*-octanol versus PBS. Samples from the *n*-octanol layer were repartitioned until consistent partition coefficient values were obtained. The measurement was done in triplicate and repeated three times.

**Biodistribution Studies.** The biodistribution experiments were performed in normal male mice (5 weeks, male, average weight, about 20 g) and approved by the Animal Care Committee of Beijing Normal University. A saline solution containing the $^{18}$F-labeled tracers (370 KBq per 100 $\mu$L) was injected directly into the tail. The mice ($n$ = 5 for each time point) were sacrificed at 2, 10, 30, and 60 min after injection. The organs of interest were removed and weighed, and radioactivity was measured with an automatic $\gamma$ counter. The percent dose per gram of wet tissue was calculated by a comparison of the tissue counts to suitably diluted aliquots of the injected material.

**In Vitro Autoradiography Studies.** Paraffin-embedded brain sections were deparaffinized with 2 × 20 min washes in xylene, 2 × 5 min washes in 100% ethanol, a 5 min wash in 90% ethanol/$H_2O$, a 5 min wash in 80% ethanol/$H_2O$, a 5 min wash in 60% ethanol/$H_2O$, and a 10 min wash in running tap water and then incubated in PBS (0.2 M, pH 7.4) for 30 min. After that, they were incubated with $^{18}$F-labeled tracers (370 KBq per 100 $\mu$L) for 1 h at room temperature. They were then washed in 40% EtOH before being rinsed with water for 1 min. After drying, the sections were exposed to a phosphorus plate (PerkinElmer, U.S.) for 2 h. In vitro autoradiographic images were obtained using a phosphor imaging system (Cyclone, Packard). After autoradiographic examination, the same mouse brain sections were stained by thioflavin S to confirm the presence of A$\beta$ plaques. For the staining of thioflavin S, sections were immersed in a 0.125% thioflavin S solution containing 10% EtOH for 3 min and washed in 40% EtOH. After drying, fluorescent observation was performed using the Oberver Z1 (Zeiss, Germany) equipped with GFP filter set (excitation, 505 nm).

**Ex Vivo Autoradiography Studies.** The ex vivo evaluation was performed using a Tg (C57BL6-APP/PS1, 10 months old, male) mouse, which was used as an Alzheimer's model, and an age-matched control (C57BL6, 10 months, male). A saline solution of the labeled agent [$^{18}$F]**32** (19.2 MBq) was injected directly into the tail vein. The mice were sacrificed by decapitation at 30 min after intravenous injection. The brains were immediately removed and frozen in a liquid nitrogen bath. Sections of 20 $\mu$m were cut and exposed to a phosphorus plate (PerkinElmer, U.S.) for 5 h. Ex vivo film autoradiograms were thus obtained using a phosphor imaging system (Cyclone, Packard). After autoradiographic examination, the same sections were stained with thioflavin S to confirm the presence of amyloid plaques.

**In Vitro Stability Studies.** The in vitro stability of [$^{18}$F]**32** in mouse plasma was determined by incubating 1.85 MBq purified [$^{18}$F]**32** with 100 $\mu$L of mouse plasma at 37 °C for 2, 10, 30, and 60 min. Proteins were precipitated by adding 200 $\mu$L of acetonitrile after centrifugation at 5000 rpm for 5 min at 4 °C. The supernatant was collected. Approximately 0.1 mL of the supernatant solution was analyzed using HPLC.

## ■ ASSOCIATED CONTENT

### Supporting Information

Purity of key target compounds together with HPLC chromatograms, $^1$H NMR spectra of compounds, and HRMS data of key target compounds. This material is available free of charge via the Internet at http://pubs.acs.org.

## ■ AUTHOR INFORMATION


### Corresponding Author

*For M.C.: phone, +86-10-58808891; fax, +86-10-58808891; e-mail, cmc@bnu.edu.cn. For B.L.: phone, +86-10-58808891; e-mail, liuboli@bnu.edu.cn.

### Author Contributions

‖These authors contributed equally.


### Notes

The authors declare no competing financial interest.

## ■ ACKNOWLEDGMENTS

The authors thank Dr. Jin Liu (College of Life Science, Beijing Normal University) for assistance in the in vitro neuropathological staining. This work was supported by National Natural Science Foundation of China (Grants 21201019, 21071023, and 30670586).

## ■ ABBREVIATIONS USED

AD, Alzheimer's disease; A$\beta$, $\beta$-amyloid; NFT, neurofibrillary tangle; CR, Congo Red; Th-T, thioflavin T; SPECT, single photon emission computed tomography; PET, positron emission tomography; IMPY, 2-(4′-dimethylaminophenyl)-6-imidazo[1,2-*a*]pyridine; PEG, polyethylene glycol; FPEG,

fluoropolyethylene glycol; THF, tetrahydrofuran; BOC, butyloxycarbonyl; TBAF, tetra-*n*-butylammonium fluoride

## REFERENCES


(1) Selkoe, D. J. The origins of Alzheimer disease: a is for amyloid. *JAMA, J. Am. Med. Assoc.* **2000**, *283*, 1615−1617.

(2) Selkoe, D. J. Alzheimer's disease: genes, proteins, and therapy. *Physiol. Rev.* **2001**, *81*, 741−766.

(3) Hardy, J.; Selkoe, D. J. The amyloid hypothesis of Alzheimer's disease: progress and problems on the road to therapeutics. *Science* **2002**, *297*, 353−356.

(4) Hardy, J. The amyloid hypothesis for Alzheimer's disease: a critical reappraisal. *J. Neurochem.* **2009**, *110*, 1129−1134.

(5) Reitz, C. Alzheimer's disease and the amyloid cascade hypothesis: a critical review. *Int. J. Alzheimer's Dis.* **2012**, *2012*, 369808.

(6) Mathis, C. A.; Wang, Y.; Klunk, W. E. Imaging $\beta$-amyloid plaques and neurofibrillary tangles in the aging human brain. *Curr. Pharm. Des.* **2004**, *10*, 1469−1492.

(7) Cai, L.; Innis, R. B.; Pike, V. W. Radioligand development for PET imaging of $\beta$-amyloid (A$\beta$)-current status. *Curr. Med. Chem.* **2007**, *14*, 19−52.

(8) Sugimoto, H. Development of anti-Alzheimer's disease drug based on $\beta$-amyloid hypothesis. *Yakugaku Zasshi* **2010**, *130*, 521−526.

(9) Valotassiou, V.; Archimandritis, S.; Sifakis, N.; Papatriantafyllou, J.; Georgoulias, P. Alzheimer's disease: spect and pet tracers for $\beta$-amyloid imaging. *Curr. Alzheimer Res.* **2010**, *7*, 477−486.

(10) Herholz, K.; Ebmeier, K. Clinical amyloid imaging in Alzheimer's disease. *Lancet Neurol.* **2011**, *10*, 667−670.

(11) Kung, M. P.; Hou, C.; Zhuang, Z. P.; Zhang, B.; Skovronsky, D.; Trojanowski, J. Q.; Lee, V. M.; Kung, H. F. IMPY: an improved thioflavin-T derivative for in vivo labeling of $\beta$-amyloid plaques. *Brain Res.* **2002**, *956*, 202−210.

(12) Zhuang, Z. P.; Kung, M. P.; Wilson, A.; Lee, C. W.; Plossl, K.; Hou, C.; Holtzman, D. M.; Kung, H. F. Structure−activity relationship of imidazo[1,2-*a*]pyridines as ligands for detecting $\beta$-amyloid plaques in the brain. *J. Med. Chem.* **2003**, *46*, 237−243.

(13) Newberg, A. B.; Wintering, N. A.; Plossl, K.; Hochold, J.; Stabin, M. G.; Watson, M.; Skovronsky, D.; Clark, C. M.; Kung, M. P.; Kung, H. F. Safety, biodistribution, and dosimetry of $^{123}$I-IMPY: a novel amyloid plaque-imaging agent for the diagnosis of Alzheimer's disease. *J. Nucl. Med.* **2006**, *47*, 748−54.

(14) Mathis, C. A.; Wang, Y.; Holt, D. P.; Huang, G. F.; Debnath, M. L.; Klunk, W. E. Synthesis and evaluation of $^{11}$C-labeled 6-substituted 2-arylbenzothiazoles as amyloid imaging agents. *J. Med. Chem.* **2003**, *46*, 2740−2754.

(15) Klunk, W. E.; Engler, H.; Nordberg, A.; Wang, Y.; Blomqvist, G.; Holt, D. P.; Bergstrom, M.; Savitcheva, I.; Huang, G. F.; Estrada, S.; Ausen, B.; Debnath, M. L.; Barletta, J.; Price, J. C.; Sandell, J.; Lopresti, B. J.; Wall, A.; Koivisto, P.; Antoni, G.; Mathis, C. A.; Langstrom, B. Imaging brain amyloid in Alzheimer's disease with Pittsburgh compound-B. *Ann. Neurol.* **2004**, *55*, 306−319.

(16) Johnson, K. A. Amyloid imaging of Alzheimer's disease using Pittsburgh compound B. *Curr. Neurol. Neurosci. Rep.* **2006**, *6*, 496−503.

(17) Johnson, A. E.; Jeppsson, F.; Sandell, J.; Wensbo, D.; Neelissen, J. A.; Jureus, A.; Strom, P.; Norman, H.; Farde, L.; Svensson, S. P. AZD2184: a radioligand for sensitive detection of $\beta$-amyloid deposits. *J. Neurochem.* **2009**, *108*, 1177−1186.

(18) Nyberg, S.; Jonhagen, M. E.; Cselenyi, Z.; Halldin, C.; Julin, P.; Olsson, H.; Freund-Levi, Y.; Andersson, J.; Varnas, K.; Svensson, S.; Farde, L. Detection of amyloid in Alzheimer's disease with positron emission tomography using [$^{11}$C]AZD2184. *Eur. J. Nucl. Med. Mol. Imaging* **2009**, *36*, 1859−1863.

(19) Ono, M.; Wilson, A.; Nobrega, J.; Westaway, D.; Verhoeff, P.; Zhuang, Z. P.; Kung, M. P.; Kung, H. F. $^{11}$C-labeled stilbene derivatives as A$\beta$-aggregate-specific PET imaging agents for Alzheimer's disease. *Nucl. Med. Biol.* **2003**, *30*, 565−571.

(20) Verhoeff, N. P.; Wilson, A. A.; Takeshita, S.; Trop, L.; Hussey, D.; Singh, K.; Kung, H. F.; Kung, M. P.; Houle, S. In-vivo imaging of Alzheimer disease $\beta$-amyloid with [$^{11}$C]SB-13 PET. *Am. J. Geriatr. Psychiatry* **2004**, *12*, 584−595.

(21) Koole, M.; Lewis, D. M.; Buckley, C.; Nelissen, N.; Vandenbulcke, M.; Brooks, D. J.; Vandenberghe, R.; Van Laere, K. Whole-body biodistribution and radiation dosimetry of 18F-GE067: a radioligand for in vivo brain amyloid imaging. *J. Nucl. Med.* **2009**, *50*, 818−22.

(22) Jureus, A.; Swahn, B. M.; Sandell, J.; Jeppsson, F.; Johnson, A. E.; Johnstrom, P.; Neelissen, J. A.; Sunnemark, D.; Farde, L.; Svensson, S. P. Characterization of AZD4694, a novel fluorinated A$\beta$ plaque neuroimaging PET radioligand. *J. Neurochem.* **2010**, *114*, 784−794.

(23) Rowe, C. C.; Ackerman, U.; Browne, W.; Mulligan, R.; Pike, K. L.; O'Keefe, G.; Tochon-Danguy, H.; Chan, G.; Berlangieri, S. U.; Jones, G.; Dickinson-Rowe, K. L.; Kung, H. P.; Zhang, W.; Kung, M. P.; Skovronsky, D.; Dyrks, T.; Holl, G.; Krause, S.; Friebe, M.; Lehman, L.; Lindemann, S.; Dinkelborg, L. M.; Masters, C. L.; Villemagne, V. L. Imaging of amyloid $\beta$ in Alzheimer's disease with 18F-BAY94-9172, a novel PET tracer: proof of mechanism. *Lancet Neurol.* **2008**, *7*, 129−135.

(24) Lin, K. J.; Hsu, W. C.; Hsiao, I. T.; Wey, S. P.; Jin, L. W.; Skovronsky, D.; Wai, Y. Y.; Chang, H. P.; Lo, C. W.; Yao, C. H.; Yen, T. C.; Kung, M. P. Whole-body biodistribution and brain PET imaging with [18F]AV-45, a novel amyloid imaging agent-a pilot study. *Nucl. Med. Biol.* **2010**, *37*, 497−508.

(25) Choi, S. R.; Golding, G.; Zhuang, Z.; Zhang, W.; Lim, N.; Hefti, F.; Benedum, T. E.; Kilbourn, M. R.; Skovronsky, D.; Kung, H. F. Preclinical properties of $^{18}$F-AV-45: a PET agent for A$\beta$ plaques in the brain. *J. Nucl. Med.* **2009**, *50*, 1887−1894.

(26) Wong, D. F.; Rosenberg, P. B.; Zhou, Y.; Kumar, A.; Raymont, V.; Ravert, H. T.; Dannals, R. F.; Nandi, A.; Brasic, J. R.; Ye, W.; Hilton, J.; Lyketsos, C.; Kung, H. F.; Joshi, A. D.; Skovronsky, D. M.; Pontecorvo, M. J. In vivo imaging of amyloid deposition in Alzheimer disease using the radioligand 18F-AV-45 (florbetapir [corrected] F 18). *J. Nucl. Med.* **2010**, *51*, 913−920.

(27) Rowe, C. C.; Villemagne, V. L. Brain amyloid imaging. *J. Nucl. Med.* **2011**, *52*, 1733−1740.

(28) Stephenson, K. A.; Chandra, R.; Zhuang, Z. P.; Hou, C.; Oya, S.; Kung, M. P.; Kung, H. F. Fluoro-pegylated (FPEG) imaging agents targeting A$\beta$ aggregates. *Bioconjugate Chem.* **2007**, *18*, 238−246.

(29) Cheng, Y.; Ono, M.; Kimura, H.; Kagawa, S.; Nishii, R.; Saji, H. A novel $^{18}$F-labeled pyridyl benzofuran derivative for imaging of $\beta$-amyloid plaques in Alzheimer's brains. *Bioorg. Med. Chem. Lett.* **2010**, *20*, 6141−6144.

(30) Ono, M.; Cheng, Y.; Kimura, H.; Cui, M.; Kagawa, S.; Nishii, R.; Saji, H. Novel $^{18}$F-labeled benzofuran derivatives with improved properties for positron emission tomography (PET) imaging of $\beta$-amyloid plaques in Alzheimer's brains. *J. Med. Chem.* **2011**, *54*, 2971−2979.

(31) Cheng, Y.; Ono, M.; Kimura, H.; Kagawa, S.; Nishii, R.; Kawashima, H.; Sajio, H. Fluorinated benzofuran derivatives for PET imaging of $\beta$-amyloid plaques in Alzheimer's disease brains. *ACS Med. Chem. Lett.* **2010**, *1*, 321−325.

(32) Cui, M.; Ono, M.; Kimura, H.; Ueda, M.; Nakamoto, Y.; Togashi, K.; Okamoto, Y.; Ihara, M.; Takahashi, R.; Liu, B.; Saji, H. Novel (18)F-labeled benzoxazole derivatives as potential positron emission tomography probes for imaging of cerebral $\beta$-amyloid plaques in Alzheimer's disease. *J. Med. Chem.* [Online early access]. DOI: 10.1021/jm300251n. Published Online: Jun 12, **2012**.

(33) Qiao, J. X.; Wang, T. C.; Hu, C.; Li, J.; Wexler, R. R.; Lam, P. Y. Transformation of anionically activated trifluoromethyl groups to heterocycles under mild aqueous conditions. *Org. Lett.* **2011**, *13*, 1804−1807.

(34) Cui, M.; Ono, M.; Kimura, H.; Kawashima, H.; Liu, B. L.; Saji, H. Radioiodinated benzimidazole derivatives as single photon emission computed tomography probes for imaging of $\beta$-amyloid plaques in Alzheimer's disease. *Nucl. Med. Biol.* **2011**, *38*, 313−320.

(35) Toyama, H.; Ye, D.; Ichise, M.; Liow, J. S.; Cai, L.; Jacobowitz, D.; Musachio, J. L.; Hong, J.; Crescenzo, M.; Tipre, D.; Lu, J. Q.; Zoghbi, S.; Vines, D. C.; Seidel, J.; Katada, K.; Green, M. V.; Pike, V.

W.; Cohen, R. M.; Innis, R. B. PET imaging of brain with the β-amyloid probe, [11C]6-OH-BTA-1, in a transgenic mouse model of Alzheimer's disease. *Eur. J. Nucl. Med. Mol. Imaging* **2005**, *32*, 593−600.
(36) Kung, H. F.; Choi, S. R.; Qu, W.; Zhang, W.; Skovronsky, D. $^{18}$F stilbenes and styrylpyridines for PET imaging of A beta plaques in Alzheimer's disease: a miniperspective. *J. Med. Chem.* **2010**, *53*, 933−941.
(37) Bonger, K. M.; van den Berg, R. J.; Heitman, L. H.; AP, I. J.; Oosterom, J.; Timmers, C. M.; Overkleeft, H. S.; van der Marel, G. A. Synthesis and evaluation of homo-bivalent GnRHR ligands. *Bioorg. Med. Chem.* **2007**, *15*, 4841−4856.
(38) Kim, D. Y.; Kim, H. J.; Yu, K. H.; Min, J. J. Synthesis of [(18)F]-labeled (2-(2-fluoroethoxy)ethyl)tris(4-methoxyphenyl)phosphonium cation as a potential agent for positron emission tomography myocardial imaging. *Nucl. Med. Biol.* **2012**, *39*, 1093−1098.
(39) Cheng, Y.; Prusoff, W. H. Relationship between the inhibition constant (K1) and the concentration of inhibitor which causes 50 per cent inhibition (I50) of an enzymatic reaction. *Biochem. Pharmacol.* **1973**, *22*, 3099−3108.
(40) Zhang, W.; Oya, S.; Kung, M. P.; Hou, C.; Maier, D. L.; Kung, H. F. F-18 polyethyleneglycol stilbenes as PET imaging agents targeting Aβ aggregates in the brain. *Nucl. Med. Biol.* **2005**, *32*, 799−809.